On The Discretization of LPV State-Space Representations

R. Tóth, P. S. C. Heuberger, P. M. J. Van den Hof

Abstract

Discretization of Linear Parameter-Varying (LPV) systems is a relevant, but insufficiently investigated problem of both LPV control design and system identification. In this contribution, existing results on the discretization of LPV state-space models with static dependence (without memory) on the scheduling signal are surveyed and new methods are introduced. These approaches are analyzed in terms of approximation error, considering ideal zero-order hold actuation and sampling of the input-output signals and scheduling variables of the system. Criteria to choose appropriate sampling periods with respect to the investigated methods are also presented. The application of the considered approaches on state-space representations with dynamic dependence (with memory) on the scheduling is investigated in a higher-order hold sense.

Index Terms

Linear parameter-varying systems; discretization; digital implementation.

I. Introduction

In the last 15 years, the field of *Linear Parameter-Varying* (LPV) systems has become a promising framework for modern industrial control with a growing number of successful applications (see [1] for a recent overview). Despite the theoretical advances of the field, implementation of LPV control designs in physical hardware often meets significant difficulties, as *continuous-time* (CT) LPV controllers [2], [3] are often preferred in practice over *discrete-time* (DT) solutions [4], [5]. The main reason is that stability and performance requirements can be more conveniently

This work was supported by the Dutch National Science Foundation (NWO).

The authors are with the Delft Center for Systems and Control. Delft University of Technology, Mekelweg 2, 2628 CD, Delft, The Netherlands, email: {r.toth,p.s.c.heuberger,p.m.j.vandenhof}@tudelft.nl.

expressed in CT, like in a mixed sensitivity setting [6]. Therefore, the current design tools focus on continuous-time LPV *State-Space* (LPV-SS) controller synthesis, requiring efficient discretization of such system representations for implementation purposes. Besides this, LPV identification methods are exclusively developed for DT. For efficient use of these approaches, structural information about the plant is required, which is often only provided by first principle CT models. These issues imply that discretization of LPV representations is a crucial issue for both identification and controller implementation.

In the early work of Apkarian [7] three different approaches for the discretization of LPV-SS representations, the *complete*, *Euler* and *Tustin* methods, were introduced (see Section III) in a *Zero-Order Hold* (ZOH) setting by extending the concepts of the *Linear Time-Invariant* (LTI) framework. However, the discussion on the discretization error and applicability of these methods for specific LPV systems was very limited. Only in [8] an attempt was made to characterize the discretization error of the Euler method in a matrix-approximation setting. Many applications of the methods introduced in [7] have been investigated with respect to *Linear Fractional Representation* (LFR) of LPV systems, [9], [10], [11], [12], even making preliminary steps towards a mixed *First-Order Hold* (1OH) discretization setting [13], [14]. However, the validity of the used discretization settings or the introduced approximation error has not been analyzed so far. As almost all of these methods suffer from various disadvantages like significant approximation errors, loss of stability, or high complexity, it is necessary to investigate the underlying approximation questions of the dynamics both in terms of numerical analysis and system stability concepts. Additionally, the complexity of the underlying problems raises the need for a useful guide to support engineers in the decision which method to use in specific situations.

In this paper, we aim to take up this challenge and complete the extension of the discretization approaches of the LTI framework to LPV state-space representations. As a main contribution, we compare the properties of the available methods with questions of sampling-period choice, preservation of stability, and discretization errors. We investigate the validity of the ZOH setting and consider when the application of a higher-order hold setting is unavoidable.

The current paper further extends the results reported in [15] and is organized as follows: first, in Section II, definitions of LPV-SS system representations are introduced. In Section III, the concept of the used ZOH setting is discussed and the discretization theory of LPV-SS

representations is reviewed, considering complete and approximative methods. In Section IV, the introduced methods are investigated in terms of discretization error and effects of sampling period choice and in Section V further properties of the approaches are presented. In Section VI it is investigated when the application of a higher-order hold discretization setting is necessary, while in Section VII a numerical example is given for the comparison of the discretization methods and the derived criteria. Finally, in Section VIII, the main conclusions of the paper are drawn.

II. LPV STATE-SPACE MODELS IN CT AND DT

In this section LPV-SS system representations are defined in CT as models of an underlying physical system $\mathcal{S}$. This concept is extended to arrive at the definition of a DT equivalent LPV-SS representation through the idea of signal sampling. In the development of the upcoming theory, we restrict the focus to LPV-SS representations with *static dependence* (without memory) on the scheduling signal, which is important since LPV-SS and LPV *Input-Output* (LPV-IO) system representations are not equivalent if static dependence on the scheduling vector is assumed, like affine dependence (see [1], [16]). Transformation between these domains depends on derivatives (CT) or time shifts (DT) of the scheduling signal (*dynamic dependence*), therefore it deforms the static dependence of the original model. Later in Section VI, the case of LPV-SS representations with dynamic dependence is revisited to investigate how the introduced theory can be applied to them.

Definition 1 (CT-LPV-SS model): Let $p_{\mathrm{c}} : \mathbb{R} \to \mathbb{P}$ be the scheduling signal of the continuous-time LPV system $\mathcal{S}$ with $\mathbb{P} \subset \mathbb{R}^{n_{\mathbb{P}}}$ a compact set called the scheduling space. The continuous-time state-space model of $\mathcal{S}$, denoted by $\mathfrak{R}^{\mathrm{c}}_{\mathrm{SS}}(\mathcal{S})$, with static scheduling dependence, is defined as

$$\dot{x}_{\mathrm{c}} = A_{\mathrm{c}}(p_{\mathrm{c}})x_{\mathrm{c}} + B_{\mathrm{c}}(p_{\mathrm{c}})u_{\mathrm{c}}, \tag{1a}$$

$$y_{\mathrm{c}} = C_{\mathrm{c}}(p_{\mathrm{c}})x_{\mathrm{c}} + D_{\mathrm{c}}(p_{\mathrm{c}})u_{\mathrm{c}}, \tag{1b}$$

where $x_{\mathrm{c}} : \mathbb{R} \to \mathbb{X} = \mathbb{R}^{n_{\mathbb{X}}}$, $u_{\mathrm{c}} : \mathbb{R} \to \mathbb{U} = \mathbb{R}^{n_{\mathbb{U}}}$ and $y_{\mathrm{c}} : \mathbb{R} \to \mathbb{Y} = \mathbb{R}^{n_{\mathbb{Y}}}$ are the state, input and output variables respectively and

$$\left[\begin{array}{c|c} A_{\mathrm{c}} & B_{\mathrm{c}} \\ \hline C_{\mathrm{c}} & D_{\mathrm{c}} \end{array}\right] : \mathbb{P} \to \left[\begin{array}{c|c} \mathbb{R}^{n_{\mathbb{X}} \times n_{\mathbb{X}}} & \mathbb{R}^{n_{\mathbb{X}} \times n_{\mathbb{U}}} \\ \hline \mathbb{R}^{n_{\mathbb{Y}} \times n_{\mathbb{X}}} & \mathbb{R}^{n_{\mathbb{Y}} \times n_{\mathbb{U}}} \end{array}\right],$$

are analytic matrix functions on $\mathbb{P}$.

By defining y_{d}, u_{d}, p_{d} as the sampled signals of y_{c}, u_{c}, p_{c} with *sampling period* $\mathtt{T}_{\mathrm{d}} > 0$, e.g., $u_{\mathrm{d}}(k) := u_{\mathrm{c}}(k\mathtt{T}_{\mathrm{d}})$, the definition of a LPV-SS representation can be established in DT as the representation of an underlying sampled continuous-time LPV system $\mathcal{S}$.

Definition 2 (DT-LPV-SS model): The p_{d}-dependent DT state-space model $\mathfrak{R}^{\mathrm{d}}_{\mathrm{SS}}(\mathcal{S}, \mathtt{T}_{\mathrm{d}})$ of $\mathcal{S}$ with discretization time $\mathtt{T}_{\mathrm{d}} > 0$ is defined as:

$$qx_{\mathrm{d}} = A_{\mathrm{d}}(p_{\mathrm{d}})x_{\mathrm{d}} + B_{\mathrm{d}}(p_{\mathrm{d}})u_{\mathrm{d}}, \tag{2a}$$

$$y_{\mathrm{d}} = C_{\mathrm{d}}(p_{\mathrm{d}})x_{\mathrm{d}} + D_{\mathrm{d}}(p_{\mathrm{d}})u_{\mathrm{d}}, \tag{2b}$$

where q is the forward time-shift operator $qx_{\mathrm{d}}(k) = x_{\mathrm{d}}(k+1)$, x_{d} is the state variable of $\mathfrak{R}^{\mathrm{d}}_{\mathrm{SS}}(\mathcal{S}, \mathtt{T}_{\mathrm{d}})$ with dimension $n_{\mathbb{X}}$, and $A_{\mathrm{d}}, \ldots, D_{\mathrm{d}}$ are bounded matrix functions on $\mathbb{P}$ with appropriate dimensions.

Note that it is not necessary that x_{d} is also a sampled version of x_{c}. Now we can define the problem we intend to focus on in the rest of the paper:

Problem 1 (Discretization problem): For a given $\mathfrak{R}^{\mathrm{c}}_{\mathrm{SS}}(\mathcal{S})$ representation of a CT-LPV system $\mathcal{S}$, investigate the possible ways of approximating with a $\mathfrak{R}^{\mathrm{d}}_{\mathrm{SS}}(\mathcal{S}, \mathtt{T}_{\mathrm{d}})$ the sampled behavior of the output signal y_{c} of $\mathcal{S}$ for all possible trajectories of the input u_{c} and the scheduling variable p_{c}. Explore the conditions on the sampling period $\mathtt{T}_{\mathrm{d}} > 0$ with respect to approximation error and preservation of stability characteristics of $\mathcal{S}$.

III. Discretization of LPV state-space models

In order to solve Problem 1, we first discuss and analyze the ZOH setting that is commonly used both in the LPV and LTI literature. Then we give a brief overview of the available extensions of LTI approaches in this setting with respect to the LPV case, also introducing two additional methods in terms of the *polynomial* and *multi-step* approaches. This overview is essential to the understanding of the upcoming numerical analysis of discretization errors and other properties in Sections IV and V.

A. Basic concepts of the discretization

In the LTI framework a great deal of research has been dedicated to discretization methods both in terms of isolated (stand-alone) and closed-loop settings [17]. Unfortunately, these approaches are not directly applicable for LPV systems due to the parameter-varying nature of the plant

(p-dependence of the system matrices). As we will see, by building on the basic concepts of LTI discretization methods, reliable LPV-SS discretization methods can still be developed.

In the available LPV discretization literature, almost exclusively an isolated approach in an ideal *Zero-Order Hold* (ZOH) setting, as presented in Figure 1, is followed where the following assumption holds:

Assumption 1 (ZOH setting): We are given a CT-LPV system $\mathcal{S}$, with CT input signal u_{c}, scheduling signal p_{c}, and output signal y_{c}, where u_{c} and p_{c} are generated by an ideal ZOH[1] device and y_{c} is sampled in a perfectly synchronized manner with $\mathtt{T}_{\mathrm{d}} > 0$ as the *sampling period* or *discretization time-step*. The ZOH and the instrument providing the output sampling have infinite resolution (no quantization error [18]) and their processing time is zero.

In terms of Assumption 1, the following relations hold for the signals of Figure 1:

$$u_{\mathrm{c}}(t) := u_{\mathrm{d}}(k), \quad \forall t \in [k\mathtt{T}_{\mathrm{d}}, (k+1)\mathtt{T}_{\mathrm{d}}), \tag{3a}$$

$$p_{\mathrm{c}}(t) := p_{\mathrm{d}}(k), \quad \forall t \in [k\mathtt{T}_{\mathrm{d}}, (k+1)\mathtt{T}_{\mathrm{d}}), \tag{3b}$$

$$y_{\mathrm{d}}(k) := y_{\mathrm{c}}(k\mathtt{T}_{\mathrm{d}}), \tag{3c}$$

for each $k \in \mathbb{Z}$, meaning that u_{c} and p_{c} can only change at the end of each sampling interval.

However in the LPV framework, this setting, i.e. Assumption 1, is criticized as, in terms of the use of LPV models, p_{c} is often considered to be a measurable external/environmental effect (general-LPV) or some function of the states, inputs, or outputs of the system $\mathcal{S}$ (quasi-LPV). Therefore, in reality it is possibly not fully influenced by the digitally controlled actuators of the plant which contain the ZOH. On the other hand, similar to the LTI case, a meaningful problem setting of discretization necessitates the restriction of the free variables of the system, i.e., u_{c} and p_{c}, to vary in a predefined manner during the sampling period. This is required in order to describe the evolution of all non-free variables inside the sampling interval, which makes it possible to derive a DT description of the system where signals are only observed at the sampling period. The simplest case is when a ZOH is applied on u_{c} and p_{c} (Assumption 1), restricting their variation to be piecewise-constant. However, this restriction can be relaxed to include a larger set of possible signal trajectories like piece-wise linear (called first-order-hold), or 2^{nd}-order polynomial (called second-order-hold), etc. Using such a setting in general can provide

[1]The ZOH device is a signal hold instrument providing a CT signal which is constant till the device is commanded to change it to a new value in a piecewise constant manner.

more accurate DT projection of the original behavior as motivated in [13], [14], however the resulting highly complicated discretization rules are likely to end up with non-causal scheduling dependence (see [19]).

By aiming at the investigation of discretization error, stability characteristics and other properties of the available LPV approaches, we also adopt the use of the LPV-ZOH setting as our basic discretization setting. We will show that this setting is only reasonable for the discretization of LPV-SS representation with static dependence as dynamic dependence requires a higher-order hold approach. The presented ZOH setting is also applicable for closed-loop controllers in the structure given in Figure 2, which has been used in [7]. Note, the assumption that the scheduling vector of the continuous LPV controller is affected by a ZOH also holds in this case.

A basic property of the LPV-ZOH setting is that, due to the assumed ideal hold devices, at the beginning of each sample interval a switching effect occurs. For the signals u_{c}, p_{c} defined through (3a-b) it holds that

$$u_{\mathrm{c}}(t) = \sum_{k=-\infty}^{\infty} 1(t - k\mathtt{T}_{\mathrm{d}}) \Big(u_{\mathrm{d}}(k) - u_{\mathrm{d}}(k-1)\Big), \tag{4a}$$

$$p_{\mathrm{c}}(t) = \sum_{k=-\infty}^{\infty} 1(t - k\mathtt{T}_{\mathrm{d}}) \Big(p_{\mathrm{d}}(k) - p_{\mathrm{d}}(k-1)\Big), \tag{4b}$$

where $1(t)$ is the unit-step function:

$$1(t) = \begin{cases} 0, & \text{if } t < 0, \\ 1, & \text{if } t \geq 0. \end{cases} \tag{5}$$

The result of $1(t - k\mathtt{T}_{\mathrm{d}})$ on $\mathfrak{R}^{\mathrm{c}}_{\mathrm{SS}}(\mathcal{S})$ in every sampling period is called the switching effect of the ZOH actuation. Contrary to the LTI case, the switching effect on p_{c} introduces additional dynamics into the system which hardly occurs in reality. Thus, to avoid the overcomplicated analysis of such effects, the following assumption is made:

Assumption 2 (Switching effects): The switching behavior of the ZOH actuation has no effect on the CT plant, i.e. the switching of the signals is assumed to take place smoothly.

Note, this assumption is automatically satisfied in most numerical simulations of LPV systems, like in the implemented numerical approaches of SIMULINK in MATLAB. The analysis of the results of this assumption is postponed till Section IV to avoid confusion. Next we summarize the approaches available in the literature and also introduce additional methods:

B. Complete method

First the LPV extension of the complete signal evolution approach [20] of the LTI framework is considered [7]. Let a CT $\mathfrak{R}^{\mathrm{c}}_{\mathrm{SS}}(\mathcal{S})$ be given in the ZOH setting. Based on Assumption 1, i.e. $p_{\mathrm{c}}(t)$ and $u_{\mathrm{c}}(t)$ are constant signals inside each sampling interval, the state-equations (1a-b) of $\mathfrak{R}^{\mathrm{c}}_{\mathrm{SS}}(\mathcal{S})$ can be written as

$$\dot{x}_{\mathrm{c}}(t) = A_{\mathrm{c}}\left(p_{\mathrm{c}}\left(k\mathtt{T}_{\mathrm{d}}\right)\right) x_{\mathrm{c}}(t) + B_{\mathrm{c}}\left(p_{\mathrm{c}}\left(k\mathtt{T}_{\mathrm{d}}\right)\right) u_{\mathrm{c}}\left(k\mathtt{T}_{\mathrm{d}}\right), \tag{6a}$$

$$y_{\mathrm{c}}(t) = C_{\mathrm{c}}\left(p_{\mathrm{c}}\left(k\mathtt{T}_{\mathrm{d}}\right)\right) x_{\mathrm{c}}(t) + D_{\mathrm{c}}\left(p_{\mathrm{c}}\left(k\mathtt{T}_{\mathrm{d}}\right)\right) u_{\mathrm{c}}\left(k\mathtt{T}_{\mathrm{d}}\right), \tag{6b}$$

for $t \in [k\mathtt{T}_{\mathrm{d}}, (k+1)\mathtt{T}_{\mathrm{d}})$ with initial condition $x_{\mathrm{c}}(k\mathtt{T}_{\mathrm{d}})$. The state equation (6a), associated with the k^{th} sampling interval, is an *Ordinary Differential Equation* (ODE). To derive a solution of this ODE, introduce $f(x_{\mathrm{c}}, u_{\mathrm{c}}, p_{\mathrm{c}})$ as the right hand side of (1a). Under Assumptions 1 and 2 it holds that

$$\int_{k\mathtt{T}_{\mathrm{d}}}^{(k+1)\mathtt{T}_{\mathrm{d}}} f(x_{\mathrm{c}}, u_{\mathrm{c}}, p_{\mathrm{c}})(\tau)\ d\tau = \int_{k\mathtt{T}_{\mathrm{d}}}^{(k+1)\mathtt{T}_{\mathrm{d}}} A_{\mathrm{c}}(p_{\mathrm{d}}(k))x_{\mathrm{c}}(\tau) + B_{\mathrm{c}}(p_{\mathrm{d}}(k))u_{\mathrm{c}}\left(k\mathtt{T}_{\mathrm{d}}\right) d\tau, \tag{7}$$

which defines the solution of (6a) at $t = (k+1)\mathtt{T}_{\mathrm{d}}$ as

$$x_{\mathrm{c}}((k+1)\mathtt{T}_{\mathrm{d}}) = x_{\mathrm{c}}(k\mathtt{T}_{\mathrm{d}}) + \int_{k\mathtt{T}_{\mathrm{d}}}^{(k+1)\mathtt{T}_{\mathrm{d}}} f(x_{\mathrm{c}}, u_{\mathrm{c}}, p_{\mathrm{c}})(\tau)\ d\tau. \tag{8}$$

Assume that $A_{\mathrm{c}}(\mathtt{p})$ is invertible[2]. By substituting $x_{\mathrm{d}}(k) = x_{\mathrm{c}}(k\mathtt{T}_{\mathrm{d}})$ and $u_{\mathrm{d}}(k) = u_{\mathrm{c}}(k\mathtt{T}_{\mathrm{d}})$, (8) gives

$$qx_{\mathrm{d}} = e^{A_{\mathrm{c}}(p_{\mathrm{d}})\mathtt{T}_{\mathrm{d}}} x_{\mathrm{d}} + A_{\mathrm{c}}^{-1}(p_{\mathrm{d}}) \left(e^{A_{\mathrm{c}}(p_{\mathrm{d}})\mathtt{T}_{\mathrm{d}}} - I\right) B_{\mathrm{c}}(p_{\mathrm{d}})\, u_{\mathrm{d}}, \tag{9a}$$

$$y_{\mathrm{d}} = C_{\mathrm{c}}(p_{\mathrm{d}})\, x_{\mathrm{d}} + D_{\mathrm{c}}(p_{\mathrm{d}})\, u_{\mathrm{d}}, \tag{9b}$$

where $y_{\mathrm{d}}(k) = y_{\mathrm{c}}(k\mathtt{T}_{\mathrm{d}})$ due to the ZOH setting. We call this discretization method the *complete method*, giving the following conversion rules:

Complete LPV-SS discretization

$$A_{\mathrm{d}}\left(p_{\mathrm{d}}(k)\right) = e^{A_{\mathrm{c}}(p_{\mathrm{c}}(k\mathtt{T}_{\mathrm{d}}))\mathtt{T}_{\mathrm{d}}}$$

$$B_{\mathrm{d}}\left(p_{\mathrm{d}}(k)\right) = A_{\mathrm{c}}^{-1}\left(p_{\mathrm{c}}(k\mathtt{T}_{\mathrm{d}})\right)\left(e^{A_{\mathrm{c}}(p_{\mathrm{c}}(k\mathtt{T}_{\mathrm{d}}))\mathtt{T}_{\mathrm{d}}} - I\right) B_{\mathrm{c}}\left(p_{\mathrm{c}}(k\mathtt{T}_{\mathrm{d}})\right)$$

$$C_{\mathrm{d}}\left(p_{\mathrm{d}}(k)\right) = C_{\mathrm{c}}\left(p_{\mathrm{c}}(k\mathtt{T}_{\mathrm{d}})\right)$$

$$D_{\mathrm{d}}\left(p_{\mathrm{d}}(k)\right) = D_{\mathrm{c}}\left(p_{\mathrm{c}}(k\mathtt{T}_{\mathrm{d}})\right)$$

[2]To compute the resulting matrix functions of this discretization approach, $A_{\mathrm{c}}(\mathtt{p})$ is not required to be invertible, but if it is, we can write the resulting DT description of the sate-evolution conveniently as (9a).

C. Approximative approaches

The complete method is commonly not favored in the LPV literature as it introduces heavy nonlinear dependence on p_{d}. Identification and control-synthesis procedures are often based on the assumption of linear, polynomial, or rational (static) dependence on p_{c}, and hence it is required to develop approximative discretization methods that try to achieve good representation of the original behavior, but with a low complexity of the coefficient dependence. To do so, the approximative discretization methods of the LTI case can be systematically extended by using different approximations of the integral that describes the state-evolution inside the sample-interval.

1) Rectangular (Euler's forward) method: The simplest way to avoid the appearance of $e^{\mathtt{T}_{\mathrm{d}}A_{\mathrm{c}}}$ is to apply a first-order approximation:

$$e^{\mathtt{T}_{\mathrm{d}}A_{\mathrm{c}}(p_{\mathrm{c}}(k\mathtt{T}_{\mathrm{d}}))} \approx I + \mathtt{T}_{\mathrm{d}}A_{\mathrm{c}}(p_{\mathrm{c}}(k\mathtt{T}_{\mathrm{d}})). \tag{10}$$

Consider $f(x_{\mathrm{c}}, u_{\mathrm{c}}, p_{\mathrm{c}})$ as defined in the previous section. Then an approximation of the solution (8) can be considered by the left-hand rectangular evaluation of (7), which gives

$$x_{\mathrm{c}}\left(\left(k+1\right)\mathtt{T}_{\mathrm{d}}\right) \approx x_{\mathrm{c}}\left(k\mathtt{T}_{\mathrm{d}}\right) + \mathtt{T}_{\mathrm{d}}A_{\mathrm{c}}\left(p_{\mathrm{c}}\left(k\mathtt{T}_{\mathrm{d}}\right)\right)x_{\mathrm{c}}\left(k\mathtt{T}_{\mathrm{d}}\right) + \mathtt{T}_{\mathrm{d}}B_{\mathrm{c}}\left(p_{\mathrm{c}}\left(k\mathtt{T}_{\mathrm{d}}\right)\right)u_{\mathrm{c}}\left(k\mathtt{T}_{\mathrm{d}}\right), \tag{11}$$

coinciding with the suggested matrix exponential approximation of (10). Based on this rectangular approach, the DT approximation of $\mathfrak{R}^{\mathrm{c}}_{\mathrm{SS}}\left(\mathcal{S}\right)$ is given by the following conversion rules:

Rectangular LPV-SS discretization

$$\begin{aligned}
A_{\mathrm{d}}\left(p_{\mathrm{d}}\left(k\right)\right) &= I + \mathtt{T}_{\mathrm{d}}A_{\mathrm{c}}\left(p_{\mathrm{c}}\left(k\mathtt{T}_{\mathrm{d}}\right)\right)\\
B_{\mathrm{d}}\left(p_{\mathrm{d}}\left(k\right)\right) &= \mathtt{T}_{\mathrm{d}}B_{\mathrm{c}}\left(p_{\mathrm{c}}\left(k\mathtt{T}_{\mathrm{d}}\right)\right)\\
C_{\mathrm{d}}\left(p_{\mathrm{d}}\left(k\right)\right) &= C_{\mathrm{c}}\left(p_{\mathrm{c}}\left(k\mathtt{T}_{\mathrm{d}}\right)\right)\\
D_{\mathrm{d}}\left(p_{\mathrm{d}}\left(k\right)\right) &= D_{\mathrm{c}}\left(p_{\mathrm{c}}\left(k\mathtt{T}_{\mathrm{d}}\right)\right)
\end{aligned}$$

Another interpretation of this method, used in [7], can be derived from *Euler's forward discretization* [21].

2) Polynomial (Hanselmann) method: It is possible to develop other methods that achieve better approximation of the complete case but with increasing complexity. As suggested in the LTI case by Hanselmann [17], one way leads trough the higher order Taylor expansion of the matrix exponential term:

$$e^{A_{\mathrm{c}}(p_{\mathrm{c}}(k\mathtt{T}_{\mathrm{d}}))\mathtt{T}_{\mathrm{d}}} \approx I + \sum_{l=1}^{n} \frac{\mathtt{T}_{\mathrm{d}}^{l}}{l!} A_{\mathrm{c}}^{l}\left(p_{\mathrm{c}}\left(k\mathtt{T}_{\mathrm{d}}\right)\right). \tag{12}$$

This results in the extension of the so called *polynomial discretization methods*. Substituting (12) into (6a) gives:

Polynomial LPV-SS discretization

$$\begin{aligned}
A_{\mathrm{d}}\left(p_{\mathrm{d}}\left(k\right)\right) &= I + \textstyle\sum_{l=1}^{n} \frac{\mathtt{T}_{\mathrm{d}}^{l}}{l!} A_{\mathrm{c}}^{l}\left(p_{\mathrm{c}}\left(k\mathtt{T}_{\mathrm{d}}\right)\right) \\
B_{\mathrm{d}}\left(p_{\mathrm{d}}\left(k\right)\right) &= \mathtt{T}_{\mathrm{d}}\left(I + \textstyle\sum_{l=1}^{n-1} \frac{\mathtt{T}_{\mathrm{d}}^{l}}{l+1!} A_{\mathrm{c}}^{l}\left(p_{\mathrm{c}}\left(k\mathtt{T}_{\mathrm{d}}\right)\right)\right) B_{\mathrm{c}}\left(p_{\mathrm{c}}\left(k\mathtt{T}_{\mathrm{d}}\right)\right) \\
C_{\mathrm{d}}\left(p_{\mathrm{d}}\left(k\right)\right) &= C_{\mathrm{c}}\left(p_{\mathrm{c}}\left(k\mathtt{T}_{\mathrm{d}}\right)\right) \\
D_{\mathrm{d}}\left(p_{\mathrm{d}}\left(k\right)\right) &= D_{\mathrm{c}}\left(p_{\mathrm{c}}\left(k\mathtt{T}_{\mathrm{d}}\right)\right)
\end{aligned}$$

3) Trapezoidal (Tustin) method: An alternative way of providing a better approximation than the rectangular method is to use a different approximative evaluation of integral (8). By using a trapezoidal evaluation, we obtain

$$x_{\mathrm{c}}\left(\left(k+1\right)\mathtt{T}_{\mathrm{d}}\right) \approx x_{\mathrm{c}}\left(k\mathtt{T}_{\mathrm{d}}\right) + \frac{\mathtt{T}_{\mathrm{d}}}{2}\Big(f|_{k\mathtt{T}_{\mathrm{d}}} + f|_{(k+1)\mathtt{T}_{\mathrm{d}}}\Big), \tag{13}$$

where $f|_{\tau} = f(x_{\mathrm{c}}, u_{\mathrm{c}}, p_{\mathrm{c}})(\tau)$. The trapezoidal approach is a commonly used technique in the LTI framework resulting in the so called *Tustin* type of discretization [22]. Furthermore, it also coincides with the *Extended Euler* method and the *1-step Adams-Moulton* method of numerical approximation of ODEs [21]. Using approximation (13), the derivation of the LPV Tustin method can be given similarly as in [7]. The key concept is to apply a change of variables:

$$\breve{x}_{\mathrm{d}}\left(k\right) = \frac{1}{\sqrt{\mathtt{T}_{\mathrm{d}}}}\left(I - \frac{\mathtt{T}_{\mathrm{d}}}{2} A_{\mathrm{c}}\left(p_{\mathrm{c}}\left(k\mathtt{T}_{\mathrm{d}}\right)\right)\right) x_{\mathrm{c}}\left(k\mathtt{T}_{\mathrm{d}}\right) - \frac{\sqrt{\mathtt{T}_{\mathrm{d}}}}{2} B_{\mathrm{c}}\left(p_{\mathrm{c}}\left(k\mathtt{T}_{\mathrm{d}}\right)\right) u_{\mathrm{d}}\left(k\right). \tag{14}$$

If $[I - \frac{\mathtt{T}_{\mathrm{d}}}{2} A_{\mathrm{c}}\left(\mathtt{p}\right)]$ is invertible for $\forall \mathtt{p} \in \mathbb{P}$, then substitution of (14) into (13) gives a DT state-equation after some algebraic manipulations. Based on this state-equation, the resulting SS representation is given by the following conversion rules:

Trapezoidal LPV-SS discretization

$$\begin{aligned}
A_{\mathrm{d}}\left(p_{\mathrm{d}}\left(k\right)\right) &= \left(I + \tfrac{\mathtt{T}_{\mathrm{d}}}{2} A_{\mathrm{c}}\left(p_{\mathrm{c}}\left(k\mathtt{T}_{\mathrm{d}}\right)\right)\right)\left(I - \tfrac{\mathtt{T}_{\mathrm{d}}}{2} A_{\mathrm{c}}\left(p_{\mathrm{c}}\left(k\mathtt{T}_{\mathrm{d}}\right)\right)\right)^{-1} \\
B_{\mathrm{d}}\left(p_{\mathrm{d}}\left(k\right)\right) &= \sqrt{\mathtt{T}_{\mathrm{d}}}\left(I - \tfrac{\mathtt{T}_{\mathrm{d}}}{2} A_{\mathrm{c}}\left(p_{\mathrm{c}}\left(k\mathtt{T}_{\mathrm{d}}\right)\right)\right)^{-1} B_{\mathrm{c}}\left(p_{\mathrm{c}}\left(k\mathtt{T}_{\mathrm{d}}\right)\right) \\
C_{\mathrm{d}}\left(p_{\mathrm{d}}\left(k\right)\right) &= \sqrt{\mathtt{T}_{\mathrm{d}}} C_{\mathrm{c}}\left(p_{\mathrm{c}}\left(k\mathtt{T}_{\mathrm{d}}\right)\right)\left(I - \tfrac{\mathtt{T}_{\mathrm{d}}}{2} A_{\mathrm{c}}\left(p_{\mathrm{c}}\left(k\mathtt{T}_{\mathrm{d}}\right)\right)\right)^{-1} \\
D_{\mathrm{d}}\left(p_{\mathrm{d}}\left(k\right)\right) &= \tfrac{\mathtt{T}_{\mathrm{d}}}{2} C_{\mathrm{c}}\left(p_{\mathrm{c}}\left(k\mathtt{T}_{\mathrm{d}}\right)\right)\left(I - \tfrac{\mathtt{T}_{\mathrm{d}}}{2} A_{\mathrm{c}}\left(p_{\mathrm{c}}\left(k\mathtt{T}_{\mathrm{d}}\right)\right)\right)^{-1} B_{\mathrm{c}}\left(p_{\mathrm{c}}\left(k\mathtt{T}_{\mathrm{d}}\right)\right) + D_{\mathrm{c}}\left(p_{\mathrm{c}}\left(k\mathtt{T}_{\mathrm{d}}\right)\right)
\end{aligned}$$

It is important to note that, like in the LTI case, the trapezoidal method approximates only the input-output behavior of $\mathfrak{R}_{\mathrm{SS}}^{\mathrm{d}}(\mathcal{S}, \mathtt{T}_{\mathrm{d}})$, as it gives an approximative DT-SS representation in terms

of a new state-variable $\breve{x}_{\mathrm{d}}$. Moreover, it is easy to show that the state transformation described by (14) is a Lyapunov transformation if $\det(I - \frac{\mathtt{T}_{\mathrm{d}}}{2} A_{\mathrm{c}}(\mathtt{p})) \neq 0$ for any $\mathtt{p} \in \mathbb{P}$ where $\mathbb{P}$ is compact. Hence it guarantees preservation of stability of the approximated system [23].

4) Multi-step methods: As an other alternative, consider the state evolution as the solution of the differential equation defined by (1a). This solution can be numerically approximated via multi-step formulas like the Runge-Kutta, Adams-Moulton, or the Adams-Bashforth type of approaches [21]. In commercial engineering software packages, like MATLAB SIMULINK, commonly variable step-size implementation of these algorithms assures accurate simulation of CT systems. However in the considered ZOH discretization setting, the step size, i.e. the sampling rate, is fixed and sampled data is only available at past and present sampling instances. This immediately excludes multi-step implicit methods like the Adams-Moulton approaches. Moreover $f(x_{\mathrm{c}}, u_{\mathrm{c}}, p_{\mathrm{c}})$ can only be evaluated for integer multiples of the sampling period, as the input only changes at these time instances and the resulting model must be realized as a single rate (not multi-rate) system. Therefore it is complicated to apply methods like the Runge-Kutta approach. The family of Adams-Bashforth methods does fulfill these requirements (see [21]). The 3-step version of this numerical approach uses the following approximation:

$$x_{\mathrm{c}}\left(\left(k+1\right)\mathtt{T}_{\mathrm{d}}\right) \approx x_{\mathrm{d}}\left(k+1\right) = x_{\mathrm{c}}\left(k\mathtt{T}_{\mathrm{d}}\right) + \frac{\mathtt{T}_{\mathrm{d}}}{12}\left(5\left.f\right|_{(k-2)\mathtt{T}_{\mathrm{d}}} - 16\left.f\right|_{(k-1)\mathtt{T}_{\mathrm{d}}} + 23\left.f\right|_{k\mathtt{T}_{\mathrm{d}}}\right). \tag{15}$$

Formulating this state-space equation in an augmented SS form with a new state-variable

$$\breve{x}_{\mathrm{d}} = \left[\begin{array}{cc} x_{\mathrm{d}}^{T} & \left.f\right|_{(k-1)\mathtt{T}_{\mathrm{d}}}^{\top} \quad \left.f\right|_{(k-2)\mathtt{T}_{\mathrm{d}}}^{\top} \end{array}\right]^{\top}, \tag{16}$$

leads to the following conversion rules:

Adams-Bashforth LPV-SS discretization

$$A_{\mathrm{d}}\left(p_{\mathrm{d}}\left(k\right)\right) = \left[\begin{array}{ccc} I + \frac{23\mathtt{T}_{\mathrm{d}}}{12} A_{\mathrm{c}}\left(p_{\mathrm{c}}\left(k\mathtt{T}_{\mathrm{d}}\right)\right) & -\frac{16\mathtt{T}_{\mathrm{d}}}{12} I & \frac{5\mathtt{T}_{\mathrm{d}}}{12} I \\ A_{\mathrm{c}}\left(p_{\mathrm{c}}\left(k\mathtt{T}_{\mathrm{d}}\right)\right) & 0 & 0 \\ 0 & I & 0 \end{array}\right]$$

$$B_{\mathrm{d}}\left(p_{\mathrm{d}}\left(k\right)\right) = \left[\begin{array}{ccc} \frac{23\mathtt{T}_{\mathrm{d}}}{12} B_{\mathrm{c}}^{T}\left(p_{\mathrm{c}}\left(k\mathtt{T}_{\mathrm{d}}\right)\right) & B_{\mathrm{c}}^{T}\left(p_{\mathrm{c}}\left(k\mathtt{T}_{\mathrm{d}}\right)\right) & 0 \end{array}\right]^{\top}$$

$$C_{\mathrm{d}}\left(p_{\mathrm{d}}\left(k\right)\right) = \left[\begin{array}{ccc} C_{\mathrm{c}}\left(p_{\mathrm{c}}\left(k\mathtt{T}_{\mathrm{d}}\right)\right) & 0 & 0 \end{array}\right]$$

$$D_{\mathrm{d}}\left(p_{\mathrm{d}}\left(k\right)\right) = D_{\mathrm{c}}\left(p_{\mathrm{c}}\left(k\mathtt{T}_{\mathrm{d}}\right)\right)$$

IV. CRITERIA AND ERRORS

As the main contribution, the previously introduced methods are investigated in terms of the generated discretization error, convergence and numerical stability, by using the tools of numerical analysis. The results of this investigation will give the basis to derive upperbounds on the sampling period $\mathtt{T}_\mathrm{d}$, that guarantee a user-defined bounded discretization error and stability preservation with respect to the original CT system. Moreover, the influence of the assumption that no switching effects result from to the ZOH actuation is investigated as well.

A. Local discretization errors

The complete method theoretically provides errorless discretization in terms of the ZOH setting. For methods that utilize an approximation, the concept of *Local Unit Truncation* (LUT) error, denoted by $\varepsilon_k \in \mathbb{R}$, is introduced. Let $R_\mathrm{x}(q, p_\mathrm{d})$ and $R_\mathrm{u}(q, p_\mathrm{d})$ be polynomials in q with p_d-dependent coefficient matrices. Choose these polynomials such that they formulate the state update of the DT approximations on the same state-basis as in $\mathfrak{R}^\mathrm{c}_\mathrm{SS}(\mathcal{S})$. In the rectangular and the polynomial case, $R_\mathrm{x}(q, p_\mathrm{d}) = A_\mathrm{d}(p_\mathrm{d})$ and $R_\mathrm{u}(q, p_\mathrm{d}) = B_\mathrm{d}(p_\mathrm{d})$, but in the other cases, they also include the appropriate state-transformation. For example in the trapezoidal case, (13) describes the DT state update with respect to the original state basis of $\mathfrak{R}^\mathrm{c}_\mathrm{SS}(\mathcal{S})$. By using the change of variables (14), we transformed (13) to correspond to an LPV state-space equation. However in terms of analysis we need to use (13) to characterize the LUT with respect to x_d. From (13) it follows that in the trapezoidal case:

$$R_\mathrm{x}(q, p_\mathrm{d})(k) = \left(I + \tfrac{\mathtt{T}_\mathrm{d}}{2} A_\mathrm{c}(p_\mathrm{d}(k))\right)\left(I - \tfrac{\mathtt{T}_\mathrm{d}}{2} A_\mathrm{c}(p_\mathrm{d}(k+1))\right)^{-1}$$

$$R_\mathrm{u}(q, p_\mathrm{d})(k) = \tfrac{\mathtt{T}_\mathrm{d}}{2}\left(I - \tfrac{\mathtt{T}_\mathrm{d}}{2} A_\mathrm{c}(p_\mathrm{d}(k+1))\right)^{-1}\left(B_\mathrm{c}(p_\mathrm{d}(k)) + B_\mathrm{c}(p_\mathrm{d}(k+1))q\right).$$

For each sampling interval, ε_k is defined by

$$T_\mathrm{d}\varepsilon_{k+n} := \left(q^n x_\mathrm{d} - R_\mathrm{x}(q, p_\mathrm{d}) x_\mathrm{d} - R_\mathrm{u}(q, p_\mathrm{d}) u_\mathrm{d}\right)(k), \tag{17}$$

where $n = 1$ for all single step methods (all considered approaches except the Adams-Bashforth case) while n equals to the number of steps in case of a multi-step methods (like $n = 3$ for the 3-step Adams-Bashforth method). Note that LUT represents the relative approximation error of the system dynamics at each sampling period, when the correct sampled continuous states x_c and inputs u_c are used for the state update of the DT system. Hence the name "local". In the

theory of numerical approximation of differential equations, ε_k is considered as the measure of accuracy [21]. The following definition is important:

Definition 3 (N-consistency, based on [21]): The discrete-time approximation of the state-equation (1a) is called numerically consistent if for any solution $(x_\mathrm{c}, p_\mathrm{c}, u_\mathrm{c})$ of (1a) it holds that

$$\lim_{\mathtt{T}_\mathrm{d}\to 0} \sup_{k\in\mathbb{Z}} \|\varepsilon_k\| = 0. \tag{18}$$

This means that - in case of N-consistency - the local approximation error reduces with decreasing $\mathtt{T}_\mathrm{d}$. However this does not imply that the supremum of the *global approximation error*,

$$\eta_{k+n} := \Big(q^n x_\mathrm{d} - R_\mathrm{x}(q, p_\mathrm{d})\hat{x}_\mathrm{d} - R_\mathrm{u}(q, p_\mathrm{d})u_\mathrm{d}\Big)(k). \tag{19}$$

where n is the number of steps in the approximation method and $\hat{x}_\mathrm{d}$ is the DT approximation of the state, decreases/converges to zero too. As a next step, the LUT error of each method is investigated together with the N-consistency.

1) Rectangular method: In this case, (17) gives

$$x_\mathrm{c}\left((k+1)\,\mathtt{T}_\mathrm{d}\right) = \Big(I + A_\mathrm{c}\left(p_\mathrm{c}\left(k\mathtt{T}_\mathrm{d}\right)\right)\mathtt{T}_\mathrm{d}\Big)x_\mathrm{c}\left(k\mathtt{T}_\mathrm{d}\right) + \mathtt{T}_\mathrm{d}B_\mathrm{c}\left(p_\mathrm{c}\left(k\mathtt{T}_\mathrm{d}\right)\right)u_\mathrm{c}\left(k\mathtt{T}_\mathrm{d}\right) + \mathtt{T}_\mathrm{d}\varepsilon_{k+1}. \tag{20}$$

Define the first-order Taylor approximation of x_c around the time-instant $k\mathtt{T}_\mathrm{d}$ as

$$x_\mathrm{c}(t) = x_\mathrm{c}(k\mathtt{T}_\mathrm{d}) + (t - k\mathtt{T}_\mathrm{d})\dot{x}_\mathrm{c}(k\mathtt{T}_\mathrm{d}) + \frac{1}{2}(t - k\mathtt{T}_\mathrm{d})^2\ddot{x}_\mathrm{c}(\tau), \tag{21}$$

for $t > k\mathtt{T}_\mathrm{d}$ and $\tau \in (k\mathtt{T}_\mathrm{d}, t)$. Substraction of (21) for $t = (k+1)\mathtt{T}_\mathrm{d}$ from (20) yields that $\mathtt{T}_\mathrm{d}\varepsilon_{k+1}$ is equal to the residual term, giving

$$\varepsilon_{k+1} = \frac{\mathtt{T}_\mathrm{d}}{2}\ddot{x}_\mathrm{c}\left(\tau\right). \tag{22}$$

with $\tau \in (k\mathtt{T}_\mathrm{d}, (k+1)\,\mathtt{T}_\mathrm{d})$. This shows that in the ZOH setting, the rectangular-method-based conversion is consistent in first order (in $\mathtt{T}_\mathrm{d}$) if $\|\ddot{x}_\mathrm{c}\left(\tau\right)\| < \infty$ for all $\tau \in \mathbb{R}$.

If f is partially differentiable[3] in each variable, then

$$\ddot{x}_\mathrm{c}(\tau) = \frac{\partial f}{\partial x_\mathrm{c}}\underbrace{\dot{x}_\mathrm{c}\left(\tau\right)}_{f|_\tau} + \frac{\partial f}{\partial u_\mathrm{c}}\dot{u}_\mathrm{c}\left(\tau\right) + \frac{\partial f}{\partial p_\mathrm{c}}\dot{p}_\mathrm{c}\left(\tau\right). \tag{23}$$

Due to Assumptions 1-2, $\dot{u}_\mathrm{c}\left(t\right) = \dot{p}_\mathrm{c}\left(t\right) = 0$ in each sampling interval. Thus, (23) gives that

$$\|\ddot{x}_\mathrm{c}\left(\tau\right)\| = \|A_\mathrm{c}\left(p_\mathrm{d}\left(k\right)\right)\, f|_\tau\| \leq \max_{\mathtt{p}\in\mathbb{P},\mathtt{x}\in\mathbb{X},\mathtt{u}\in\mathbb{U}} \left\|A_\mathrm{c}^2\left(\mathtt{p}\right)\mathtt{x} + A_\mathrm{c}\left(\mathtt{p}\right)B_\mathrm{c}\left(\mathtt{p}\right)\mathtt{u}\right\|, \tag{24}$$

[3]In the general LPV setting, the system matrices of (1a) are not necessary partially differentiable in p_c.

	Rectangular	n^{th}-polynomial	Trapezoidal	Adams-Bashforth (3-step)
ε_k	$\frac{\mathtt{T}_\mathrm{d}}{2} x_\mathrm{c}^{(2)}(\tau)$	$\frac{\mathtt{T}_\mathrm{d}^n}{(n+1)!} x_\mathrm{c}^{(n+1)}(\tau)$	$\frac{1}{12}\mathtt{T}_\mathrm{d}^2 x_\mathrm{c}^{(3)}(\tau)$	$\frac{3}{8}\mathtt{T}_\mathrm{d}^3 x_\mathrm{c}^{(4)}(\tau)$
$\breve{\mathtt{T}}_\mathrm{d}$	$\min\limits_{\mathtt{p}\in\mathbb{P}} \min\limits_{\lambda\in\sigma(A_\mathrm{c}(\mathtt{p}))} -\frac{2\mathrm{Re}(\lambda)}{\lvert\lambda\rvert^2}$	$\arg\min\limits_{\mathtt{T}_\mathrm{d}\in\mathbb{R}_0^+} \left\lvert \max\limits_{\mathtt{p}\in\mathbb{P}} \bar{\sigma}\left(\sum\limits_{l=0}^{n} \frac{\mathtt{T}_\mathrm{d}^l}{l!} A_\mathrm{c}^l(\mathtt{p})\right) - 1 \right\rvert$	$\max\limits_{\mathtt{p}\in\mathbb{P}} \max\limits_{\substack{\lambda\in\sigma(A_\mathrm{c}(\mathtt{p}))\\ \mathrm{Im}(\lambda)=0}} \frac{2}{\mathrm{Re}(\lambda)}$	$\arg\min\limits_{\mathtt{T}_\mathrm{d}\in\mathbb{R}_0^+} \left\lvert \max\limits_{\bar{\mathtt{p}}\in\mathbb{P}^n} \bar{\lambda}\left(R_{\bar{\mathtt{p}}}(z,\mathtt{T}_\mathrm{d})\right) - 1 \right\rvert$
$\hat{\mathtt{T}}_\mathrm{d}$	$\sqrt{2\frac{\varepsilon_{\max} M_\mathtt{x}^{\max}}{100 M^{(1)}}}$	$\sqrt[n+1]{\frac{\varepsilon_{\max} M_\mathtt{x}^{\max}(n+1)!}{100 M^{(n)}}}$	$\sqrt[3]{\frac{12\varepsilon_{\max} M_\mathtt{x}^{\max}}{100 M^{(2)}}}$	$\sqrt[4]{\frac{8\varepsilon_{\max} M_\mathtt{x}^{\max}}{300 M^{(3)}}}$

TABLE I

LOCAL TRUNCATION ERROR ε_k WITH $\tau \in (k\mathtt{T}_\mathrm{d}, (k+1)\mathtt{T}_\mathrm{d})$ AND WITH $\tau \in ((k-2)\mathtt{T}_\mathrm{d}, (k+1)\mathtt{T}_\mathrm{d})$ IN THE ADAMS-BASHFORTH CASE, SAMPLING BOUNDARY OF STABILITY $\breve{\mathtt{T}}_\mathrm{d}$, AND SAMPLING UPPERBOUND OF PERFORMANCE $\hat{\mathtt{T}}_\mathrm{d}$ OF LPV-SS ZOH DISCRETIZATION METHODS.

where $\|\,\mathbf{.}\,\|$ is an arbitrary norm. Note in (24), that $\mathbb{X}$ and $\mathbb{U}$ must be bounded sets to be able to compute this upperbound. If this is not the case, then commonly $\mathbb{X}$ and $\mathbb{U}$ can be restricted to a bounded subset corresponding to the image of the typical trajectories of the system variables. Then the previous bound can be formulated for this region of interest. In the sequel we denote this upperbound by $M^{(1)}$ and call it the first-order *numerical sensitivity* (N-sensitivity) constant. Note that $M^{(1)}$ can be approximated through gridding to derive an estimate. Using similar arguments, the LUT error of other discretization methods can be formulated. The results are given in the first row of Table I, showing that each method is consistent with varying orders. Here $x_\mathrm{c}^{(n)}$ denotes the $n^{\text{th}}-$order derivative of the continuous state signal. Moreover, using (23) and the chain rule of differentiation, higher order sensitivity constants can be derived:

$$M^{(n)} = \max_{\mathtt{p}\in\mathbb{P},\mathtt{x}\in\mathbb{X},\mathtt{u}\in\mathbb{U}} \left\| A_\mathrm{c}^{n+1}(\mathtt{p})\,\mathtt{x} + A_\mathrm{c}^{n}(\mathtt{p})\,B_\mathrm{c}(\mathtt{p})\,\mathtt{u} \right\|.$$

The derived results can also be compared with the existing error characterization of the rectangular method given in [8]. In this work an upperbound on the matrix approximation error of (10) has been introduced using basic algebra. This bound describes the discretization error also in the local sense, however it can not directly describe the approximation error of the state evolution. The latter is necessary to derive useful criteria for choosing adequate sampling periods (see Section IV-C). Therefore, the error concept of [8] is not considered here.

B. Global convergence and preservation of stability

So far only the LUT error of the introduced methods has been investigated, giving basic proofs of consistency. As a next step we investigate global convergence of approximative methods

together with their *numerical stability* (N-stability). The latter concept means that small errors in the initial condition of the discrete-time approximation do not cause the solution to diverge. As an important result we show that for the single-step approximative discretization methods, N-stability is identical with the preservation of the uniform frozen stability of the original representation. In this context, uniform frozen stability means the stability of the LPV system (in terms of bounded solutions) for each constant trajectory of p. The relation we show between the stability concepts means that, in case of numerical stability, the discretization method does not changes the frozen stability of the discretized model, which is a prime requirement of a successful DT approximation of a CT system. To derive adequate criteria for the largest sampling period for which this property holds (N-stability radius), each method is analyzed and computable formulas are derived.

Let $\mathbb{Z}^+ = \{\mathtt{x} \in \mathbb{Z} \mid \mathtt{x} > 0\}$ and $\mathbb{Z}_0^- = \mathbb{Z} \setminus \mathbb{Z}^+$. According to the previously explained line of discussion, we introduce the following concepts:

Definition 4 (N-convergence, based on [21]): Let $\mathfrak{R}^{\mathrm{c}}_{\mathrm{SS}}(\mathcal{S})$ be the CT representation of the LPV system $\mathcal{S}$ with state-signal x_{c} and let $\hat{x}_{\mathrm{d}}$ denote the DT approximation of x_{c} with a discretization method using $\mathtt{T}_{\mathrm{d}} > 0$. Then a discretization method is called numerically convergent, if for any state trajectory x_{c} of $\mathfrak{R}^{\mathrm{c}}_{\mathrm{SS}}(\mathcal{S})$, the approximation $\hat{x}_{\mathrm{d}}$ satisfies that

$$\lim_{\mathtt{T}_{\mathrm{d}} \to 0} \sup_{k \in \mathbb{Z}_0^-} \|\hat{x}_{\mathrm{d}}(k) - x_{\mathrm{c}}(k\mathtt{T}_{\mathrm{d}})\| = 0 \quad \Rightarrow \quad \lim_{\mathtt{T}_{\mathrm{d}} \to 0} \sup_{k \in \mathbb{Z}^+} \|\hat{x}_{\mathrm{d}}(k) - x_{\mathrm{c}}(k\mathtt{T}_{\mathrm{d}})\| = 0. \tag{25}$$

Note that in the trapezoidal and multi-step cases, $\hat{x}_{\mathrm{d}}$ is the appropriate transform of $\breve{x}_{\mathrm{d}}$ with respect to x_{c}. In terms of Definition 4, N-convergence means that the discretized solution of the state-equation can get arbitrary close to the original CT behavior by decreasing $\mathtt{T}_{\mathrm{d}}$ (see Figure 3).

Definition 5 (N-stability, based on [21]): A discretization method is called numerically stable if, for sufficiently small values of $\mathtt{T}_{\mathrm{d}}$ and ϵ, any two state-trajectories $\hat{x}_{\mathrm{d}}$, $\hat{x}'_{\mathrm{d}}$ of the discretized representation associated with the same input-output and scheduling trajectory on the half-line $\mathbb{Z}^+$, satisfy that $\|\hat{x}_{\mathrm{d}}(0) - \hat{x}'_{\mathrm{d}}(0)\| < \epsilon$ implies the existence of a $\gamma \geq 0$ such that $\|\hat{x}_{\mathrm{d}}(k) - \hat{x}'_{\mathrm{d}}(k)\| < \gamma\epsilon$, $\forall k \in \mathbb{Z}^+$.

The notion of N-stability means that small errors in the initial condition will not cause divergence as the solution is iterated (see Figure 4). For the approximative methods, N-convergence and N-stability are questions of main importance. To be able to analyze these nummerical notions

for the introduced discretization approaches, first consider the single-step methods. Introduce the characteristic polynomial $R_{\mathtt{p}}(q, \mathtt{T}_{\mathrm{d}})$ of the frozen aspects of the discretized SS representation as

$$R_{\mathtt{p}}(q, \mathtt{T}_{\mathrm{d}}) = \det(qI - A_{\mathrm{d}}(\mathtt{p})), \tag{26}$$

where $\mathtt{p} \in \mathbb{P}$ and q is the forward time-shift operator. Due to the multi-step nature of the Adams-Bashforth method - to avoid conservatism of the upcoming analysis - $R_{\mathtt{p}}$ is defined to reflect the multi-step nature of the state evolution. In the n-step Adams-Bashforth case, the state evolution with respect to discretized original state x_{d} is characterized by

$$q^n I - \mathtt{T}_{\mathrm{d}} \sum_{l=0}^{n-1} \gamma_l q^l A_{\mathrm{c}}, \tag{27}$$

with $\{\gamma_l\}_{l=0}^{n-1} \subset \mathbb{R}$ the Adams-Bashforth approximation coefficients (values of these coefficients for $n > 0$ are given in [21]). The form of (27) results due to the augmented state vector $\breve{x}_{\mathrm{d}}$ (see (16)). Note that multiplication of A_{c} by the time operator q^l is non-commutative, i.e. $q^l A_{\mathrm{c}}(p_{\mathrm{d}}(k)) = A_{\mathrm{c}}(p_{\mathrm{d}}(k+l))q^l \neq A_{\mathrm{c}}(p_{\mathrm{d}}(k))q^l$. Thus, even if $\mathfrak{R}^{\mathrm{c}}_{\mathrm{SS}}(\mathcal{S})$ has static dependence, the resulting polynomial in (27) becomes dynamically dependent on p_{d}. To express this, the following local characteristic polynomial is introduced in the "frozen" sense for a scheduling sequence $\bar{\mathtt{p}} = [\ \mathtt{p}_0 \quad \dots \quad \mathtt{p}_{n-1}\ ] \in \mathbb{P}^n$:

$$R_{\bar{\mathtt{p}}}(q, \mathtt{T}_{\mathrm{d}}) = \det\left(q^n I - \mathtt{T}_{\mathrm{d}} \sum_{l=0}^{n-1} \gamma_l A_{\mathrm{c}}(\mathtt{p}_l) q^l\right), \tag{28}$$

Now it is possible to substitute q with the Z-transform $z \in \mathbb{C}$ to formulate the characteristic polynomial in the frequency domain. This provides the following theorem to characterize N-stability of the introduced discretization methods:

Theorem 1 (Strong root-condition): Discretization methods are N-convergent and N-stable if, for all $\lambda \in \mathbb{C}$ with

$$\exists \mathtt{p}_0, \dots \mathtt{p}_{n-1} \in \mathbb{P} \text{ such that } R_{\bar{\mathtt{p}}}(\lambda, 0) = 0, \tag{29}$$

it holds that $|\lambda| \leq 1$ and if $|\lambda| = 1$, then $\frac{\partial}{\partial \lambda} R_{\bar{\mathtt{p}}}(\lambda, 0) \neq 0$.

The proof of this theorem follows similarly as in [21] and it can be shown that all of the introduced LPV-SS discretization methods satisfy it. Based on the strong-root condition it is possible to compute an exact upperbound $\breve{T}_{\mathrm{d}}$ of the "sufficiently small" $\mathtt{T}_{\mathrm{d}}$ that provides N-stability:

Definition 6 (N-stability-radius): The N-stability radius $\breve{\mathtt{T}}_{\mathrm{d}}$ is defined as the largest $\mathtt{T}_{\mathrm{d}} \in \mathbb{R}_0^+$ such that for any $\mathtt{p}_0, \dots, \mathtt{p}_{n-1} \in \mathbb{P}$, all roots $\lambda \in \mathbb{C}$ of $R_{\bar{\mathtt{p}}}(\lambda, \mathtt{T}_{\mathrm{d}})$ satisfy that $|\lambda| \leq 1$.

Definition 6 has an interesting consequence for the discretization of LPV-SS representations. Namely that, through the characteristic polynomial $R_{\bar{\mathtt{p}}}$, it implies that, if $\mathtt{T}_\mathrm{d} < \breve{\mathtt{T}}_\mathrm{d}$, then in the single-step cases the resulting DT representation defines a uniformly frozen stable system, as for this $\mathtt{T}_\mathrm{d}$ it is satisfied that

$$\max_{\mathtt{p}\in\mathbb{P}} \ \bar{\sigma}\left(A_\mathrm{d}\left(\mathtt{p}\right)\right) \leq 1, \tag{30}$$

where $\bar{\sigma}\left(\centerdot\right) = \max\left|\sigma\left(\centerdot\right)\right|$ is the spectral radius and $\sigma\left(\centerdot\right)$ is the eigenvalue operator. If the original CT system $\mathcal{S}$ is globally stable (quadratic, BIBO, etc.), then it is commonly desirable that its DT approximation is also globally stable. For such a property it is needed that uniform frozen stability of $\mathfrak{R}^\mathrm{c}_\mathrm{SS}\left(\mathcal{S}\right)$:

$$\max_{\mathtt{p}\in\mathbb{P}} \max_{\lambda\in\sigma(A_\mathrm{c}(\mathtt{p}))} \mathrm{Re}\{\lambda\} \leq 0, \tag{31}$$

is preserved, resulting in the uniform frozen stability of the DT representation. It follows that for the introduced single-step discretization methods preservation of local stability of the original system and N-stability of the discretization method both require local stability of the resulting DT representation. For N-stability it is a sufficient, for preservation of global stability of $\mathcal{S}$ it is a necessary condition.

In case of the rectangular method, (30) is equivalent with

$$\max_{\mathtt{p}\in\mathbb{P}} \ \bar{\sigma}\left(I + \mathtt{T}_\mathrm{d} A_\mathrm{c}\left(\mathtt{p}\right)\right) \leq 1. \tag{32}$$

Due to the basic properties of eigenvalues, it can be shown that (32) holds iff

$$\max_{\mathtt{p}\in\mathbb{P}} \max_{\lambda\in\sigma(A_\mathrm{c}(\mathtt{p}))} \left|\tfrac{1}{\mathtt{T}_\mathrm{d}} + \lambda\right| \leq \tfrac{1}{\mathtt{T}_\mathrm{d}}. \tag{33}$$

From (33), the stability radius is

$$\breve{\mathtt{T}}_\mathrm{d} = \max\left(0, \ \min_{\mathtt{p}\in\mathbb{P}} \min_{\lambda\in\sigma(A_\mathrm{c}(\mathtt{p}))} -\frac{2\mathrm{Re}\left(\lambda\right)}{\left|\lambda\right|^2}\right). \tag{34}$$

Note that $\breve{\mathtt{T}}_\mathrm{d} = 0$ in case of non-uniformly frozen stable $\mathfrak{R}^\mathrm{c}_\mathrm{SS}\left(\mathcal{S}\right)$, meaning that the rectangular DT approximation of a non-uniformly frozen stable system is not N-stable. Computation of the bound (34) is a nonlinear optimization problem for which an approximative solution may follow by the gridding of $\mathbb{P}$.

In case of the polynomial method, (30) translates to

$$\max_{\mathtt{p}\in\mathbb{P}} \ \bar{\sigma}\left(I + \sum_{l=1}^{n} \tfrac{\mathtt{T}_\mathrm{d}^l}{l!} A_\mathrm{c}^l\left(\mathtt{p}\right)\right) < 1. \tag{35}$$

From (35), the stability radius reads as

$$\breve{\mathtt{T}}_{\mathrm{d}} = \arg\min_{\mathtt{T}_{\mathrm{d}} \in \mathbb{R}_0^+} \left| \max_{\mathtt{p} \in \mathbb{P}} \bar{\sigma} \left(\sum_{l=0}^{n} \frac{\mathtt{T}_{\mathrm{d}}^l}{l!} A_{\mathrm{c}}^l (\mathtt{p}) \right) - 1 \right|. \tag{36}$$

Again, an approximation of $\breve{\mathtt{T}}_{\mathrm{d}}$ can be given by applying bisection-based search in $\mathtt{T}_{\mathrm{d}}$ on (36) over a grid of $\mathbb{P}$. In case of non-uniform frozen stability, $\breve{\mathtt{T}}_{\mathrm{d}} = 0$ with this method as well.

For the trapezoidal method, condition (30) becomes quite complicated due to the inverse term $\left[I - \frac{\mathtt{T}_{\mathrm{d}}}{2} A_{\mathrm{c}} (p_{\mathrm{d}}) \right]^{-1}$ in $A_{\mathrm{d}} (p_{\mathrm{d}})$. First it must be guaranteed that this inverse exists for all scheduling signals, meaning that

$$\det \left(I - \tfrac{\mathtt{T}_{\mathrm{d}}}{2} A_{\mathrm{c}} (\mathtt{p}) \right) \neq 0, \quad \forall \mathtt{p} \in \mathbb{P}, \tag{37}$$

or equivalently

$$\min_{\mathtt{p} \in \mathbb{P}} \underline{\sigma} \left(I - \tfrac{\mathtt{T}_{\mathrm{d}}}{2} A_{\mathrm{c}} (\mathtt{p}) \right) > 0, \tag{38}$$

where $\underline{\sigma} (\centerdot) = \min |\sigma (\centerdot)|$. Again, the eigenvalue properties yield that (38) equals to

$$\min_{\mathtt{p} \in \mathbb{P}} \min_{\lambda \in \sigma(A_{\mathrm{c}}(\mathtt{p}))} \left| \tfrac{2}{\mathtt{T}_{\mathrm{d}}} - \lambda \right| > 0,$$

which is guaranteed, for every $0 \leq \mathtt{T}_{\mathrm{d}} < \breve{\mathtt{T}}_{\mathrm{d}}$, where

$$\breve{\mathtt{T}}_{\mathrm{d}} = \max_{\mathtt{p} \in \mathbb{P}} \max_{\substack{\lambda \in \sigma(A_{\mathrm{c}}(\mathtt{p})) \\ \mathrm{Im}(\lambda) = 0}} \frac{2}{\mathrm{Re} (\lambda)}. \tag{39}$$

Instead of convergence, here $\breve{\mathtt{T}}_{\mathrm{d}}$ ensures the existence of the DT projection (existence of A_{d}). It is shown later that, if the DT projection exists, then N-convergence holds. Note that, in case $\mathrm{Im} (\lambda) \neq 0$ for all $\lambda \in \sigma (A_{\mathrm{c}} (\mathtt{p}))$ and $\mathtt{p} \in \mathbb{P}$, meaning that every frozen representation of the original CT system has only complex poles, condition (38) is guaranteed for arbitrary $\mathtt{T}_{\mathrm{d}}$, resulting in $\breve{\mathtt{T}}_{\mathrm{d}} = \infty$. Similarly, uniform frozen stability of $\mathfrak{R}_{\mathrm{SS}}^{\mathrm{c}} (\mathcal{S})$, meaning that every frozen representation has poles with only negative or zero real part, gives $\breve{\mathtt{T}}_{\mathrm{d}} = \infty$. In [7], the condition

$$\mathtt{T}_{\mathrm{d}} \leq \max_{\mathtt{p} \in \mathbb{P}} \frac{2}{\bar{\sigma} \left(A_{\mathrm{c}} (\mathtt{p}) \right)}, \tag{40}$$

was proposed to guarantee invertibility, which is a rather conservative upperbound of (39). If $0 \leq \mathtt{T}_{\mathrm{d}} < \breve{\mathtt{T}}_{\mathrm{d}}$ holds and $\mathfrak{R}_{\mathrm{SS}}^{\mathrm{c}} (\mathcal{S})$ has uniform frozen stability, then (31) is satisfied, as

$$\max_{\mathtt{p} \in \mathbb{P}} \bar{\sigma} \left(\left[I + \frac{\mathtt{T}_{\mathrm{d}}}{2} A_{\mathrm{c}} (\mathtt{p}) \right] \left[I - \frac{\mathtt{T}_{\mathrm{d}}}{2} A_{\mathrm{c}} (\mathtt{p}) \right]^{-1} \right) \leq 1. \tag{41}$$

Thus, for stable LPV-SS systems, the trapezoidal method always guarantees N-stability and N-convergence if $\mathtt{T}_{\mathrm{d}}$ satisfies condition (39).

In case of the Adams-Bashforth method, the concept of N-stability means that

$$\max_{\bar{\mathtt{p}}\in\mathbb{P}^n} \bar{\lambda}\left(R_{\bar{\mathtt{p}}}\left(z,\mathtt{T}_\mathrm{d}\right)\right) \leq 1, \tag{42}$$

where $\bar{\lambda}\left(R(z)\right) = \max_{\lambda\in\mathbb{C},\, R(\lambda)=0} |\lambda|$. A necessary condition for (42) is that the resulting DT representation has uniform frozen stability:

$$\max_{\bar{\mathtt{p}}\in\mathbb{P}^n} \bar{\sigma}\left(A_\mathrm{d}\left(\mathtt{p}\right)\right) \leq 1. \tag{43}$$

This means that in the multi-step case, preservation of frozen stability is not sufficient to imply N-stability. From (42) it follows that the N-stability radius reads as

$$\breve{\mathtt{T}}_\mathrm{d} = \underset{\mathtt{T}_\mathrm{d}\in\mathbb{R}_0^+}{\arg\min} \left| \max_{\bar{\mathtt{p}}\in\mathbb{P}^n} \bar{\lambda}\left(R_{\bar{\mathtt{p}}}(z,\mathtt{T}_\mathrm{d})\right) - 1 \right|, \tag{44}$$

which is a too complicated expression to be further analyzed. However, in practice it can be solved based on gridding and bisection based search.

C. Adequate discretization step size

In the previous part we have investigated the numerical properties of the introduced discretization methods. However, the appropriate choice of $\mathtt{T}_\mathrm{d}$ to arrive at a specific performance in terms of discretization error is also important from a practical point of view. By using the LUT error expressions developed in Section IV-A, upperbounds of $\mathtt{T}_\mathrm{d}$ are derived that guarantee a certain bound on the approximation error in terms of a chosen measure $\|\centerdot\|$. Define ε_* as the supremum of $\|\varepsilon_k\|$ over all possible state trajectories of $\mathfrak{R}^\mathrm{c}_\mathrm{SS}(\mathcal{S})$ and $k \in \mathbb{Z}$. Also introduce

$$M^{\max}_{\mathtt{x}} = \sup_{x_\mathrm{c}} \max_{t\in\mathbb{R}} \|x_\mathrm{c}\left(t\right)\| = \max_{\mathtt{x}\in\mathbb{X}} \|\mathtt{x}\|, \tag{45}$$

as the maximum "amplitude" of the state signal for any u_c and p_c. Also define $\varepsilon_{\max}$ as the required maximum relative local error of the discretization in terms of percentage. Then a $\mathtt{T}_\mathrm{d} > 0$ is searched for that satisfies

$$\varepsilon_* \leq \frac{\varepsilon_{\max} M^{\max}_{\mathtt{x}}}{100 \cdot \mathtt{T}_\mathrm{d}}. \tag{46}$$

Next we formulate an upperbound of $\mathtt{T}_\mathrm{d}$ with respect to each method, such that (46) is satisfied for the desired $\varepsilon_{\max}$ percentage. Note that, to derive these criteria, (45) must be bounded, i.e. $\mathbb{X}$ must be confined in a ball (bounded region) of $\mathbb{R}^{n_\mathbb{X}}$, which is not a unrealistic assumption in case of global asymptotic stability of $\mathcal{S}$ and bounded $\mathbb{P}$ and $\mathbb{U}$.

Based on (22), it holds in the rectangular case that

$$\varepsilon_* = \sup_{x_\mathrm{c}} \sup_{\tau\in\mathbb{R}} \tfrac{\mathtt{T}_\mathrm{d}}{2} \left\|\ddot{x}_\mathrm{c}\left(\tau\right)\right\|. \tag{47}$$

By using the sensitivity constant $M^{(1)} \geq \sup \|\ddot{x}_{\mathrm{c}}(\tau)\|$, inequality (47) holds for any $0 \leq \mathtt{T}_{\mathrm{d}} \leq \hat{\mathtt{T}}_{\mathrm{d}}$ where

$$\hat{\mathtt{T}}_{\mathrm{d}} = \sqrt{2\frac{\varepsilon_{\max} M_{\mathbf{x}}^{\max}}{100 \cdot M^{(1)}}}. \tag{48}$$

Criterion (48) provides an upperbound estimate of the required $\mathtt{T}_{\mathrm{d}}$, that achieves $\varepsilon_{\max}$ percentage local discretization error of the state variable in terms of a chosen measure. Similar criteria can be developed for the other methods by using the LUT error expressions of Table I and the higher-order sensitivity constants $M^{(n)}$. These upperbounds are presented in the third row of Table I.

In practical situations one may be concerned about the maximum of the global error η_k (see (19)) as a performance measure. Define η_* as the supremum of $\|\eta_k\|$ over all possible state trajectories of $\mathfrak{R}_{\mathrm{SS}}^{\mathrm{c}}(\mathcal{S})$ and $k \in \mathbb{Z}$. Also define $\eta_{\max}$ as the maximal acceptable relative global error of the discretization in terms of percentage. Then one would like to choose $\mathtt{T}_{\mathrm{d}}$ such that

$$\eta_* \leq \frac{\eta_{\max} M_{\mathbf{x}}^{\max}}{100}. \tag{49}$$

Unfortunately, characterization of η_* for the introduced discretization methods requires serious restrictions on the considered CT behaviors. However, in case of $\mathtt{T}_{\mathrm{d}} \leq \breve{\mathtt{T}}_{\mathrm{d}}$, $\varepsilon_{\max}$ can be used as a good approximation of $\eta_{\max}$, and therefore the performance bound $\hat{\mathtt{T}}_{\mathrm{d}}$ can be used to bound the global error as well (see Section VII).

D. Switching effects

In the previous part the effect of neglecting the switching phenomena of the ZOH actuation has not been considered. Here we investigate the case when the signals u_{c} and p_{c} described by (3a-b) are applied to $\mathfrak{R}_{\mathrm{SS}}^{\mathrm{c}}(\mathcal{S})$. Consider the ODE corresponding to (1a) in the k^{th} sample interval. By using the bilateral Laplace transform of (1a) with reference time $t_0 = k\mathtt{T}_{\mathrm{d}}$ and assuming that the dependence on p_{c} is commutative under addition[4], it follows that

$$\begin{aligned} sX(s) = x_{\mathrm{c}}(k\mathtt{T}_{\mathrm{d}}) + \left(\tfrac{A_{\mathrm{c}}(p_{\mathrm{c}}(k\mathtt{T}_{\mathrm{d}})) + (s-1)A_{\mathrm{c}}(p_{\mathrm{c}}((k-1)\mathtt{T}_{\mathrm{d}}))}{s}\right) X(s) \\ + \tfrac{B_{\mathrm{c}}(p_{\mathrm{c}}(k\mathtt{T}_{\mathrm{d}}))}{s} u_{\mathrm{c}}(k\mathtt{T}_{\mathrm{d}}) + \left(\tfrac{(s-1)B_{\mathrm{c}}(p_{\mathrm{c}}((k-1)\mathtt{T}_{\mathrm{d}}))}{s}\right) u_{\mathrm{c}}((k-1)\mathtt{T}_{\mathrm{d}}), \end{aligned} \tag{50}$$

[4]Without this assumption the formulation of the Laplace transform becomes complicated, but the core problem that results in the general case is illustrated by (50).

for a fixed k, where $X(s)$ is the Laplace transform of the solution of the ODE (the behavior of the state in the k^{th} sample interval). On the contrary of the effect of the switching phenomena in the LTI case, the underlying system of (50) does not correspond to (2a) nor it is realizable as a LPV-SS system with static dependence without the introduction of virtual input and scheduling terms corresponding to $u_{\text{d}}(k-1)$ and $p_{\text{d}}(k-1)$. This way it becomes clear that neglecting the switching effects introduces discretization errors in the LPV case which can be even more significant if $\mathtt{T}_{\text{d}}$ is decreased (more discontinuous switches in the dynamics). On the other hand it is true that the discontinuous phenomena which are described by (50) never happen in reality. One reason is that usually p_{c} is not actuated by ZOH and it changes smoothly and relatively slowly with respect to the actual dynamics of the plant. Additionally, the ZOH actuation has a transient as the underlying physical device needs to build up the new signal value, preventing sudden changes of the signals. In conclusion, for LPV systems, the introduced discretization methods of this paper provide no step-invariant discretization in the ZOH setting (meaning equivalence even in case of switching effects), however they provide well-applicable methods for practical use. It is important to note that derivation of LPV discretization methods with step-invariant property is also possible, however the resulting discretization approaches are complicated and their actual performance gain compared to the previously developed approaches is insignificant in practice.

V. Properties of the approaches

Beside stability and discretization-error characteristics there are other properties of the derived discretization methods which could assist or hinder further use of the derived DT model. With the previously derived results, these vital properties are summarized in Table II. From this table it is apparent that the complete method provides errorless conversion at the price of heavy nonlinear dependence of the DT model on p_{d}. As in LPV control synthesis mostly low complexity dependence (like linear, polynomial, or rational functions) is assumed (see [3]), therefore both for modeling and controller-discretization purposes – beside the preservation of stability – the preservation of linear dependence over the scheduling is also highly preferred. This favors approximative methods that give acceptable performance, but with less complexity of the new coefficient dependence on the scheduling. Complicated dependence on p_{d}, like inversion or matrix exponential, also results in a serious increase of the computation time, which gives a preference towards the linear methods like the rectangular or the Adams-Bashforth approach. In

Property	Complete	Rectangular	n^{th}-polynomial	Trapezoidal	n-step Adams-Bashforth
consistency / convergence	always	1^{st}-order	n^{th}-order	2^{nd}-order	n^{th}-order
preservation of stability / N-stab.	always global	frozen with $\breve{\mathrm{T}}_{\mathrm{d}}$	frozen with $\breve{\mathrm{T}}_{\mathrm{d}}$	always frozen	frozen with $\breve{\mathrm{T}}_{\mathrm{d}}$
preservation of instability	+	-	-	+	-
existence	always	always	always	conditional	always
complexity	exponential	linear	polynomial	rational	linear
preservation of affine dependence	-	+	-	-	+
computational load	high	low	moderate	high	low
system order	preserved	preserved	preserved	preserved	increased

TABLE II

PROPERTIES OF THE DERIVED DISCRETIZATION METHODS

the latter case, discretization also results in the order increase of the DT system which requires extra memory storage or more complicated controller design depending on the intended use. If the quality of the DT model has priority, then the trapezoidal and the polynomial methods are suggested due to their fast convergence and large stability radius. In terms of identification, linear dependence of the suggested model structure is also important as it simplifies parametrization.

VI. HIGHER-ORDER-HOLDS AND DISCRETIZATION WITH DYNAMIC DEPENDENCE

In the previous sections, the discretization problem of LPV-SS representations with static dependence has been investigated in a ZOH setting. We could see that this setting allows the use of simple discretization rules and also to design the introduced discretization error. However, the natural question that rises is how can we do better by considering a higher order-hold setting, what price we must pay for the increased accuracy and when the use of such a setting is unavoidable. This is what we intend to investigate next.

In LPV system theory equivalence transformation between representation domains results in dynamic dependence [16], [1], [24]. A CT-LPV representation with dynamic dependence has coefficients that are functions of p_{c} and its derivatives $\dot{p}_{\mathrm{c}}, \ddot{p}_{\mathrm{c}}, \ldots$, while in DT, dynamic dependence means that the coefficients are functions of $\ldots, p_{\mathrm{d}}(k-1), p_{\mathrm{d}}(k), p_{\mathrm{d}}(k+1), \ldots$. In [16], [24] it has been shown that LPV-IO representations with static dependence have LPV-SS realizations with dynamic dependence. Additionally, often first-principle nonlinear models offer a structure to rewrite them as an LPV system with dependence on a signal and its derivatives

[1]. Neglecting this dynamic dependence by the introduction of virtual scheduling signals for the derivative terms can introduce serious conservatism into the model. Thus, dynamic dependence is a real phenomenon and should be treated accordingly in LPV discretization as well.

Using the previously investigated discretization approaches on systems with dynamic dependence and assuming that the scheduling varies in a piecewise-constant manner can introduce serious conservatism. Consider the case when $A_{\mathrm{c}}(p_{\mathrm{c}}, \dot{p}_{\mathrm{c}}) = \alpha p_{\mathrm{c}} \dot{p}_{\mathrm{c}}$ with $\alpha \in \mathbb{R}$. Then in the ZOH setting (Assumption 1), the following holds in each sample interval:

$$A_{\mathrm{c}}(p_{\mathrm{c}}(t), \dot{p}_{\mathrm{c}}(t)) = \begin{cases} 0, & \text{if } t \neq k\mathtt{T}_{\mathrm{d}},\ k \in \mathbb{Z}; \\ \pm\infty, & \text{if } t = k\mathtt{T}_{\mathrm{d}},\ k \in \mathbb{Z}. \end{cases} \tag{51}$$

If the switching effect is neglected (Assumption 2), then A_{c} is approximated in DT as a identity matrix by all of the introduced discretization methods. However in practice, one would try to use the approximation

$$\dot{p}_{\mathrm{c}}(t) \approx \frac{p_{\mathrm{c}}((k+1)\mathtt{T}_{\mathrm{d}}) - p_{\mathrm{c}}(k\mathtt{T}_{\mathrm{d}})}{\mathtt{T}_{\mathrm{d}}} \tag{52}$$

for each $t \in [k\mathtt{T}_{\mathrm{d}}, (k+1)\mathtt{T}_{\mathrm{d}})$. In fact, (51) means that p_{c} is assumed to be a linear function in the sample interval. By using this assumption a better DT approximation of the original CT representation can be achieved. This shows that, in case of dynamic dependence, the ZOH assumption on p_{c} is not appropriate and, instead of that, a first or higher order hold discretization is necessary for the scheduling variable.

Based on the previous example, consider the case when $(u_{\mathrm{c}}, y_{\mathrm{c}})$ are assumed to satisfy the ZOH setting, but p_{c} varies linearly in each sampling interval $t \in [k\mathtt{T}_{\mathrm{d}}, (k+1)\mathtt{T}_{\mathrm{d}}))$:

$$p_{\mathrm{c}}(t) = \underbrace{\tfrac{p_{\mathrm{d}}(k+1) - p_{\mathrm{d}}(k)}{\mathtt{T}_{\mathrm{d}}}}_{\mathtt{p}_{1k}}(t - k\mathtt{T}_{\mathrm{d}}) + p_{\mathrm{d}}(k). \tag{53}$$

This assumption on the scheduling is called the *first-order hold* setting. Additionally, define $\mathtt{p}_{0k} = (k+1)p_{\mathrm{d}}(k) - kp_{\mathrm{d}}(k+1)$. Note that, $p_{\mathrm{c}}(t) = \mathtt{p}_{1k}t + \mathtt{p}_{0k}$ for $t \in [k\mathtt{T}_{\mathrm{d}}, (k+1)\mathtt{T}_{\mathrm{d}}))$. Let $\mathfrak{R}^{\mathrm{c}}_{\mathrm{SS}}(\mathcal{S})$ be a continuous-time SS representation and consider it in the above defined setting. In case the system matrices of $\mathfrak{R}^{\mathrm{c}}_{\mathrm{SS}}(\mathcal{S})$ are dependent on p_{c} and $\dot{p}_{\mathrm{c}}$ (dynamic dependence), then the state-evolution in the k^{th} sampling interval satisfies:

$$\dot{x}_{\mathrm{c}}(t) = A_{\mathrm{c}}(\mathtt{p}_{1k}t + \mathtt{p}_{0k}, \mathtt{p}_{1\mathtt{k}})x_{\mathrm{c}}(t) + B_{\mathrm{c}}(\mathtt{p}_{1k}t + \mathtt{p}_{0k}, \mathtt{p}_{1\mathtt{k}})\mathtt{u}_k,$$

where $\mathtt{u}_k = u(k\mathtt{T}_{\mathrm{d}})$. The solution of this ODE can be obtained for a particular function of A_{c} and B_{c}. Similar to the complete method of the ZOH setting in Section III-B, this analytical solution

results in a complete type of discretization of the continuous-time LPV-SS representation and can be also used for higher-accuracy discretization of representations with static dependence. However, the resulting DT counterpart via this projection has dynamic dependence on $p_{\mathrm{d}}(k) = p_{\mathrm{c}}(k\mathtt{T}_{\mathrm{d}})$ and its time-shifted versions disregarding that the original description had static or dynamic dependence. On the other hand, such a projection trivially yields a better approximation of the CT representation than what would result in a pure ZOH setting. This suggests the following conclusions:

1) For the discretization of LPV representations with dynamic dependence, the order of the hold setting with respect to p_{c} should be greater or equal than the maximal order of derivatives in the coefficient dependencies.
2) Applying a higher-order setting results in dynamic dependence of the resulting DT description which may even be non-causal. This is in accordance with the observations of [13].

With some trivial modifications, the approximative methods treated in this paper, except the trapezoidal method, can be extended to this hybrid higher-order hold case, but the exact formulation of these extensions is not considered here. Unfortunately, for the extended approaches, the deduced formulas for the approximation error and the step-size bounds do not apply. Solving discretization of LPV representations with dynamic dependence in a general sense and giving compact formulas of discretization for higher-order settings remains the objective of further research.

VII. Numerical example

In this section, a simple example is presented to visualize/compare the properties of the analyzed discretization methods and the performance of the sample-bound criteria. Consider the following state-space representation of a continuous-time SISO LPV system $\mathcal{S}$:

$$\mathfrak{R}^{\mathrm{c}}_{\mathrm{SS}}(\mathcal{S}) = \left[\begin{array}{cc|c} 19.98p_{\mathrm{c}} - 20 & 202 - 182p_{\mathrm{c}} & 1 + p_{\mathrm{c}} \\ 45p_{\mathrm{c}} - 50 & 0 & 1 + p_{\mathrm{c}} \\ \hline 1 + p_{\mathrm{c}} & 1 + p_{\mathrm{c}} & \frac{1+p_{\mathrm{c}}}{10} \end{array}\right]$$

where $\mathbb{P} = [-1, 1]$. The above representation has static linear dependence on p_{c}. Furthermore, for a constant scheduling $p_{\mathrm{c}}(t) = \mathtt{p}$ for all $t \in \mathbb{R}$, $\mathfrak{R}^{\mathrm{c}}_{\mathrm{SS}}(\mathcal{S})$ is equivalent with an LTI representation

that has poles

$$9.99\mathtt{p} - 10 \pm \mathrm{i}\sqrt{10^4 - 17990.2\mathtt{p} + 8090.2\mathtt{p}^2},$$

which implies that $\mathcal{S}$ is uniformly frozen stable on $\mathbb{P}$.

Assume that $\mathcal{S}$ is in a ZOH setting with sampling rate $\mathtt{T}_\mathrm{d} = 0.02$. By applying the discretization methods of Section III, approximative discrete-time representations of $\mathcal{S}$ have been calculated. To show the performance of the investigated discretization methods, the output of the original and its DT approximations have been simulated on the $[0, 1]$ time interval for zero initial conditions and for 100 different realizations of white u_d and p_d with uniform distribution $\mathcal{U}(-1, 1)$. For fair comparison, the achieved average MSE[5] of the resulting output signals $\hat{y}_\mathrm{d}$ has been calculated[6] with respect to the output y_c of $\mathfrak{R}^\mathrm{c}_\mathrm{SS}(\mathcal{S})$ and presented in Table III. The relative worst-case maximum global error $\hat{\eta}_\mathrm{max} = 100 \cdot \eta_* / M^\mathrm{max}_\mathtt{x}$ of the DT state-signals $\hat{x}_\mathrm{d}$ associated with the DT representations has been also computed with respect to x_c of $\mathfrak{R}^\mathrm{c}_\mathrm{SS}(\mathcal{S})$ and presented in Table III. From these error measures it is immediate that, except for the complete and the trapezoidal method, all approximations diverge. As expected, the error of the complete method is extremely small and the trapezoidal method gives a moderate, but acceptable performance.

As a second step, we calculate sampling bounds $\breve{\mathtt{T}}_\mathrm{d}$ and $\hat{\mathtt{T}}_\mathrm{d}$ by choosing the Euclidian norm as an error measure and $\varepsilon_\mathrm{max} = 1\%$, with the intention to achieve $\eta_\mathrm{max} = 1\%$. The calculated sampling bounds are presented in Table IV. During the calculation of $\hat{\mathtt{T}}_\mathrm{d}$ it has been assumed that $\mathbb{X} = [-0.1, 0.1]^2$, which has been verified by several simulations of $\mathfrak{R}^\mathrm{c}_\mathrm{SS}(\mathcal{S})$ based on $u_\mathrm{d}, p_\mathrm{d} \in \mathcal{U}(-1, 1)$. By these results, the rectangular method needs a fast sampling rate to achieve a stable projection and even a faster sampling to obtain the required performance. The 2^nd-order polynomial projection has significantly better bounds due to the 2^nd-order accuracy of this method. For the trapezoidal case, the existence of the transformation is always guaranteed because $\mathfrak{R}^\mathrm{c}_\mathrm{SS}(\mathcal{S})$ is uniformly frozen stable. For comparison, the bound of [7] given by (40), gives $\breve{\mathtt{T}}_\mathrm{d} = 0.2$.

Now the derived bounds are used to choose a $\mathtt{T}_\mathrm{d}$ for the calculation of the discrete projections. As the $\breve{\mathtt{T}}_\mathrm{d}$ bounds of Table IV represent the boundary of stability, therefore $\mathtt{T}_\mathrm{d} < \breve{\mathtt{T}}_\mathrm{d}$ is used as

[5]*Mean Squared Error*: expected value of the squared estimation error: $\bar{\mathcal{E}}\left\{(y_\mathrm{c} - \hat{y}_\mathrm{d})^2\right\} = \lim_{N\to\infty} \frac{1}{N} \sum_{k=0}^{N-1} \left(y_\mathrm{c}\left(k\mathtt{T}_\mathrm{d}\right) - \hat{y}_\mathrm{d}\left(k\right)\right)^2$, where $\bar{\mathcal{E}}$ is the generalized expectation operator.

[6]The response of $\mathfrak{R}^\mathrm{c}_\mathrm{SS}(\mathcal{S})$ has been calculated via a 5^th-order Runge-Kutta numerical approximation (see [21]) with step size 10^{-8}. Thus, the switching effect of the ZOH actuation does not show up in the calculated response.

MSE of y_{d}

$\mathtt{T}_{\mathrm{d}}$	Complete	Rectangular	2^{nd}-polynom.	Trapezoidal	3-step Adams-Bash.
$2 \cdot 10^{-2}$, (50Hz)	$1.68 \cdot 10^{-10}$	$(*)$	$(*)$	$1.97 \cdot 10^{-3}$	$(*)$
$5 \cdot 10^{-3}$, (0.2kHz)	$1.69 \cdot 10^{-10}$	$(*)$	$4.70 \cdot 10^{-4}$	$3.81 \cdot 10^{-5}$	$2.14 \cdot 10^{-1}$
10^{-4}, (10kHz)	$1.68 \cdot 10^{-10}$	$2.27 \cdot 10^{-6}$	$1.05 \cdot 10^{-10}$	$1.53 \cdot 10^{-8}$	$1.6 \cdot 10^{-8}$

$\hat{\eta}_{\max}$ of $\hat{x}_{\mathrm{d}}$

$\mathtt{T}_{\mathrm{d}}$	Complete	Rectangular	2^{nd}-polynom.	Trapezoidal	3-step Adams-Bash.
$2 \cdot 10^{-2}$, (50Hz)	0.053%	$(*)$	$(*)$	106.12%	$(*)$
$5 \cdot 10^{-3}$, (0.2kHz)	0.060%	$(*)$	40.31%	8.02%	665.94%
10^{-4}, (10kHz)	0.063%	2.62%	0.06%	0.19%	0.76%

TABLE III

DISCRETIZATION ERROR OF $\mathcal{S}$, GIVEN IN TERMS OF THE ACHIEVED AVERAGE MSE AND $\hat{\eta}_{\max}$ FOR 100 SIMULATIONS. $(*)$ INDICATES UNSTABLE PROJECTION TO THE DISCRETE DOMAIN.

Criteria

	Rectangular	2^{nd}-polynomial	Trapezoidal	3-step Adams-Bash.
$\breve{\mathtt{T}}_{\mathrm{d}}$	$2 \cdot 10^{-4}$, (5kHz)	$5.60 \cdot 10^{-3}$, (0.2kHz)	∞	$1.77 \cdot 10^{-3}$, (0.6kHz)
$\hat{\mathtt{T}}_{\mathrm{d}}$	$6.87 \cdot 10^{-5}$, (15kHz)	$1.73 \cdot 10^{-3}$, (0.6kHz)	$1.28 \cdot 10^{-3}$, (0.8kHz)	$1.21 \cdot 10^{-3}$, (0.8kHz)

TABLE IV

STABILITY ($\breve{\mathtt{T}}_{\mathrm{d}}$) AND PERFORMANCE ($\hat{\mathtt{T}}_{\mathrm{d}}$) BOUNDS PROVIDED BY THE CRITERION FUNCTIONS OF TABLE I USING THE EUCLIDIAN NORM AND $\varepsilon_{\max} = 1\%$.

a new sampling period in each case. Discretization of $\mathfrak{R}^{\mathrm{c}}_{\mathrm{SS}}(\mathcal{S})$ with $\mathtt{T}_{\mathrm{d}} = 0.005$, almost the stability bound of the polynomial method, provides the simulation results given in the second row of Table III. The rectangular method again results in an unstable projection, while the Adams-Bashforth method is on the brink of instability due to frozen instability of A_{d} for some $\mathtt{p} \in \mathbb{P}$. The polynomial method gives a stable, convergent approximation, in accordance with its $\breve{\mathtt{T}}_{\mathrm{d}}$ bound. The trapezoidal method also improves significantly in performance. The achieved $\hat{\eta}_{\max}$ of each approximative method is above the aimed 1% which is in accordance with their $\hat{\mathtt{T}}_{\mathrm{d}}$.

As a next step, discretizations of $\mathfrak{R}^{\mathrm{c}}_{\mathrm{SS}}(\mathcal{S})$ with $\mathtt{T}_{\mathrm{d}} = 10^{-4}$, the half of the $\breve{\mathtt{T}}_{\mathrm{d}}$ bound of the rectangular method, are calculated. The results are given in the third row of Table III.

Finally, the rectangular method converges and also the approximation capabilities of the other methods improve. By looking at the achieved $\hat{\eta}_{\max}$, all the methods, except the rectangular, obtain the aimed 1% error performance which is in accordance with their $\hat{\mathrm{T}}_{\mathrm{d}}$ bound, while in the rectangular case the achieved $\hat{\eta}_{\max}$ is larger than 1% as 10^{-4} is larger than its $\hat{\mathrm{T}}_{\mathrm{d}}$ bound. An interesting phenomenon is that the approximation error of the complete method is non-zero and it is slightly increasing by lowering the sampling period. This increasing approximation error is due to numerical errors of the digital computation. However, the resulting approximation error is significantly less than the step size of the numerical approximation used for the simulation of $\mathfrak{R}^{\mathrm{c}}_{\mathrm{SS}}(\mathcal{S})$, thus it can be considered zero.

VIII. Conclusion

In this paper the properties of the extension of ZOH-based isolated discretization approaches to the LPV state-space case have been investigated, under the assumption that the state-space matrices have static dependence on the scheduling signal. The concepts of local unit truncation error, numerical convergence and stability of the approximations of the original CT behavior have been analyzed, together with the preservation of uniform frozen stability. Using the results of these investigations, practically applicable conditions for the choice of the sampling period have been derived and a comparison of the methods in terms of various properties has been given. An illustrative example has also been provided to give insight into the derived methods and their conditions. It has been shown that for the discretization of LPV state-space systems with dynamic dependence a higher-order hold setting is required for the scheduling signal. Using such a setting for improving the accuracy of the discretization of models with static dependence results in dynamic dependence of the discrete-time counterparts. Extending the derived approaches to such a higher-order hold discretization setting and understanding the numerical properties of such methods will be the objective of future research.

References

[1] R. Tóth, "Modeling and identification of linear parameter-varying systems, an orthonormal basis function approach," Ph.D. dissertation, Delft University of Technology, 2008.

[2] A. Packard and G. Becker, "Quadratic stabilization of parametrically-dependent linear system using parametrically-dependent linear, dynamic feedback," *Advances in Robust and Nonlinear Control Systems*, vol. DSC, no. 43, pp. 29–36, 1992.

[3] C. W. Scherer, "Mixed $\mathcal{H}_2/\mathcal{H}_\infty$ control for time-varying and linear parametrically-varying systems," *Int. Journal of Robust and Nonlinear Control*, vol. 6, no. 9-10, pp. 929–952, 1996.

[4] P. Apkarian and P. Gahinet, "A convex characterization of gain-scheduled $\mathcal{H}_\infty$ controllers," *IEEE Trans. on Automatic Control*, vol. 40, no. 5, pp. 853–864, 1995.

[5] A. Packard, "Gain scheduling via linear fractional transformations," *Systems & Control Letters*, vol. 22, no. 2, pp. 79–92, 1994.

[6] K. Zhou and J. C. Doyle, *Essentials of Robust Control*. Prentice-Hall, 1998.

[7] P. Apkarian, "On the discretization of LMI-synthesized linear parameter-varying controllers," *Automatica*, vol. 33, no. 4, pp. 655–661, 1997.

[8] R. Hallouzi, M. Verhaegen, and S. Kanev, "Model weight estimation for FDI using convex fault models," in *Proc. of the 6th IFAC Symposium on Fault Detection, Supervision and Safety of Technical Processes*, Beijing, China, Aug. 2006, pp. 795–800.

[9] J. Kim, D. G. Bates, and I. Postletwaite, "Robustness analysis of linear periodic time-varying systems subject to structured uncertainty," *Systems & Control Letters*, vol. 55, pp. 719–725, 2006.

[10] L. Ma and P. Iglesias, "Robustness analysis of a self-oscillating molecular network in a dictyostelium discoideum," in *Proc. of the 41th IEEE Conf. on Decision and Control*, Las Vegas, Nevada, USA, Dec. 2002, pp. 2538–2543.

[11] P. C. Pellanda, P. Apkarian, and H. D. Tuan, "Missile autopilot design via a multi-channel LFT/LPV control method," *Int. Journal of Robust and Nonlinear Control*, vol. 12, no. 1, pp. 1–20, 2002.

[12] G. Ferreres, "Reduction of dynamic LFT systems with LTI model uncertainties," *Int. Journal of Robust and Nonlinear Control*, vol. 14, no. 3, pp. 307–323, 2004.

[13] D. Peaucelle, C. Farges, and D. Arzelier, "Robust LFR-based technique for stability analysis of limit cycles," in *Proc. of the IFAC Symposium ALCOSP'07/PSYCO'07*, St. Petersburg, Russia, Aug. 2007.

[14] N. Imbert, "Robustness analysis of a launcher attitude controller via μ-analysis," in *Proc. of the 15th IFAC Symposium on Automatic Control in Aerospace*, Bologna, Italy, Sept. 2001, pp. 429–434.

[15] R. Tóth, F. Felici, P. S. C. Heuberger, and P. M. J. Van den Hof, "Crucial aspects of zero-order-hold LPV state-space system discretization," in *Proc. of the 17th IFAC World Congress*, Seoul, Korea, July 2008, pp. 3246–3251.

[16] ——, "Discrete time LPV I/O and state space representations, differences of behavior and pitfalls of interpolation," in *Proc. of the European Control Conf.*, Kos, Greece, July 2007, pp. 5418–5425.

[17] H. Hanselmann, "Implementation of digital controllers - A survey," *Automatica*, vol. 23, no. 1, pp. 7–32, 1987.

[18] R. M. Gray and D. L. Neuhoff, "Quantization," *IEEE Trans. on Information Theory*, vol. 44, no. 6, pp. 2325–2383, 1998.

[19] R. Tóth, M. Lovera, P. S. C. Heuberger, and P. M. J. Van den Hof, "Discretization of linear fractional representation of LPV systems: approaches and performance," *In prep.*, 2009.

[20] K. J. Åström and B. Wittenmark, *Computer controlled systems*. Prentice-Hall, 1990.

[21] K. E. Atkinson, *An Introduction to Numerical Analysis*. John Wiley and Sons, 1989.

[22] R. H. Middleton and G. C. Goodwin, *Digital control and estimation - A unified approach*. Prentice-Hall, 1990.

[23] R. E. Kalman, "Mathematical description of linear dynamical systems," *SIAM Journal on Control*, vol. 1, pp. 152–192, 1963.

[24] R. Tóth, J. C. Willems, P. S. C. Heuberger, and P. M. J. Van den Hof, "A behavioral approach to LPV systems," in *Proc. of the European Control Conf.*, Budapest, Hungary, Aug. 2009, pp. 2015–2020.

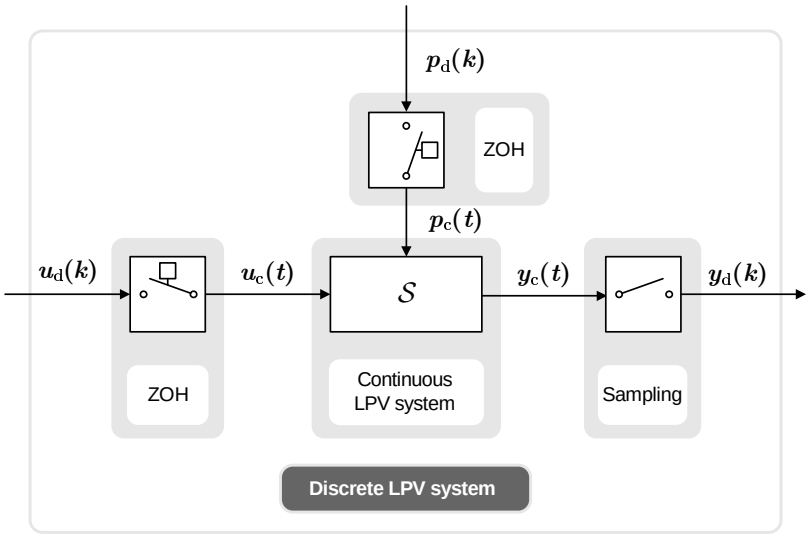

Fig. 1. Ideal zero-order hold discretization setting of general LPV systems.

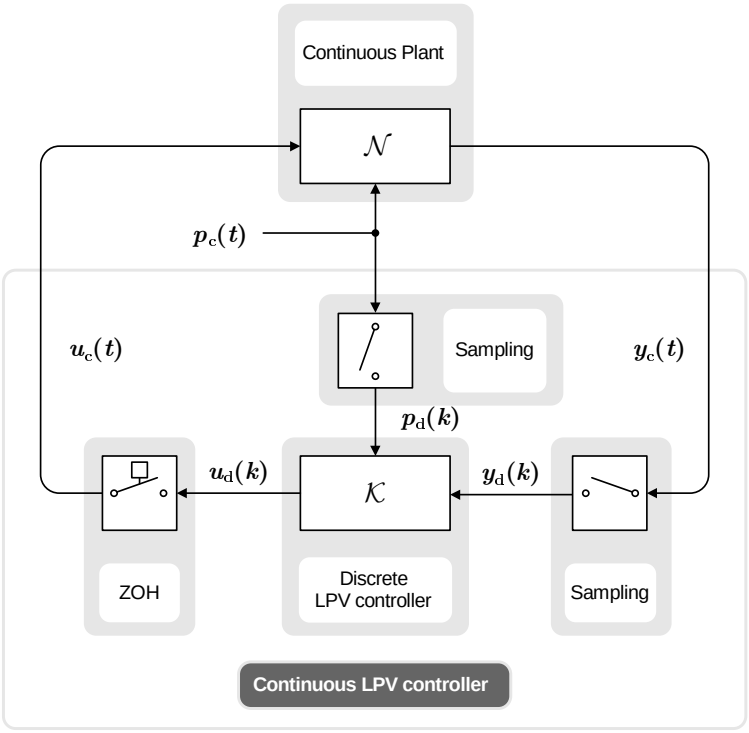

Fig. 2. Ideal ZOH discretization setting of closed-loop LPV controllers.

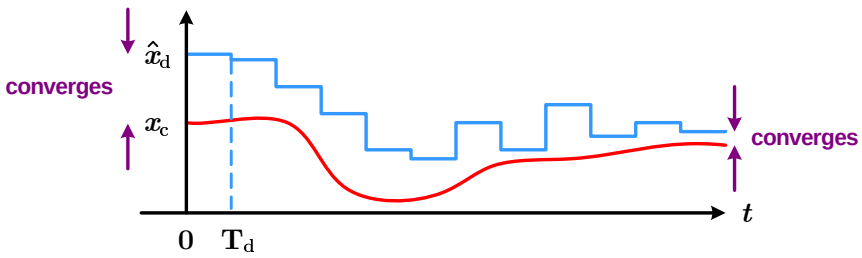

Fig. 3. N-convergence of the DT approximation. The DT state-signal $\hat{x}_{\mathrm{d}}$ converges to the CT state-signal x_{c} of the approximated representation, if the error on the initial conditions (past) of the approximation converges to zero.

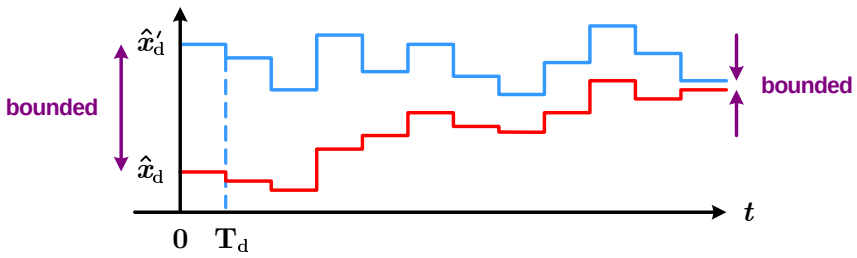

Fig. 4. N-stability of the DT approximation. Let $\hat{x}_{\mathrm{d}}$ and $\hat{x}'_{\mathrm{d}}$ be two state trajectories provided by the approximation method for the same input and scheduling on the half line $\mathbb{Z}^+$. If the difference between the initial conditions of $\hat{x}_{\mathrm{d}}$ and $\hat{x}'_{\mathrm{d}}$ is bounded, then the difference of the two trajectories on $\mathbb{Z}^+$ is also bounded.

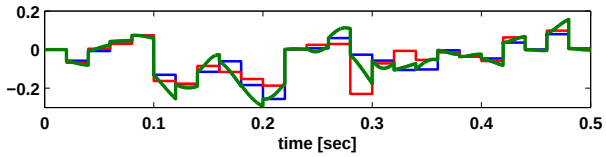

(a) $\mathtt{T}_\mathrm{d} = 0.02$, complete (blue), trapezoidal (red)

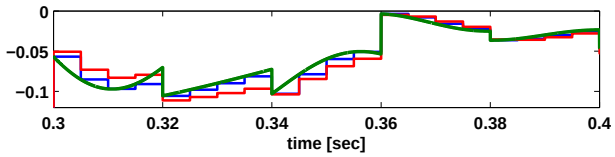

(b) $\mathtt{T}_\mathrm{d} = 0.005$, complete (blue), trapezoidal (red)

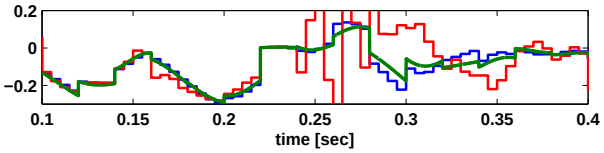

(c) $\mathtt{T}_\mathrm{d} = 0.005$, 2^{nd} order polynomial (blue), Adams-Bashforth (red)

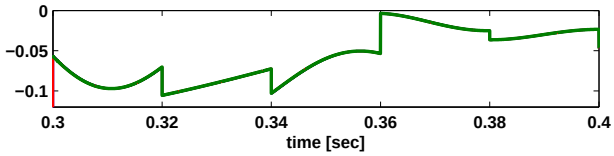

(d) $\mathtt{T}_\mathrm{d} = 10^{-4}$, complete (blue), trapezoidal (red)

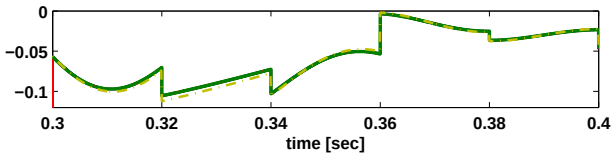

(e) $\mathtt{T}_\mathrm{d} = 10^{-4}$, 2^{nd} order polynomial (blue), Adams-Bashforth (red), rectangular (dash-dotted yellow)

Fig. 5. Output signal y_c of $\mathfrak{R}^\mathrm{c}_{\mathrm{SS}}(\mathcal{S})$ (green) in a ZOH setting with $\mathtt{T}_\mathrm{d} = 0.02$ and its discrete-time approximations with different sampling periods.